OTKA-K 101793

FINAL REPORT

Investigating the role of small regulatory RNAs in temperature sensing in *Arabidopsis*

György Szittya PhD

National Agricultural Research and Innovation Centre
Agricultural Biotechnology Institute
Institute of Plant Biotechnology

23.12.2016

Abbreviations:

AGO: Argonaute protein
A. thaliana: Arabidopsis thaliana
DCL: DICER-LIKE
N. benthamiana: Nicotiana benthamiana
mRNA: messenger RNA
miRNA: microRNA
pha-siRNA: phased siRNA
PolIV: RNA polymerase IV
PolV: RNA polymerase V
RDR: RNA Dependent RNA Polymerase
RITS complex: RNA Induced Transcriptional Silencing complex
ROS1: REPRESSOR OF SILENCING
sRNA: small RNA
siRNA: short interfering RNA
ta-siRNA: trans-acting siRNA
WT: wild type

Summary

Plants as sessile organisms continually sense and adapt to environmental conditions. The 21-24 nt small regulatory RNAs (sRNA) have recently been recognised as important gene expression regulators, which play a major role in development and adaptation. However, little is known about how they respond to ambient temperature at the genomic level. It was shown recently, that chromatin state is important to mediate thermosensory response in plants. Since sRNAs are important chromatin regulators in plants, it was plausible to hypothesize that sRNAs could have a role in temperature sensing and mediating physiological responses to different temperature.

To profile changes in temperature regulated mRNA and sRNA expression, we have grown *A. thaliana* Col-0 plants at three different ambient temperatures (15, 21 or 27 °C). We used Illumina deep-sequencing platform followed by computational methods to identify, profile and describe conserved and non-conserved sRNAs during different ambient temperature conditions. Furthermore we also identified sRNA cleaved mRNAs through genomic-scale high-throughput Illumina sequencing. During our analysis we found many sRNA loci with temperature dependent expression pattern and most of them were located in transposons or intergenic regions. In our sRNA libraries we identified 28 miRNA families and 378 different miRNA sequences. We identified 187 miRNA/cleavage target pairs using degradome libraries prepared from four tissues and three temperatures. We identified the mRNAs that were cleaved by the temperature regulated miRNAs. Among the experimentally identified targets we found significant enrichment for the GO terms of nucleic acid binding, DNA binding, transcription regulator activity and transcription factor activity. These findings may suggest that the temperature regulated miRNAs serves as master regulators in temperature dependent gene expression regulation. One of the temperature regulated miRNAs belongs to the miR169

family. The NF-YA2 component of the SOC1 regulating NF-Y TF complex is regulated by miR169h-n. The SOC1 floral pathway integrator triggers the floral transition during plant development under environmental conditions that are favourable for reproduction. Based on our work we propose that miR169h-n could mediate ambient temperature signals during inductive photoperiod to modify flowering time via SOC1.

In our sRNA libraries we also identified pha-siRNA loci that were temperature regulated. We identified the mRNAs that were cleaved by the temperature regulated pha-siRNAs in our degradome libraries. Among the experimentally identified targets we found significant enrichment for the GO terms of post-embryonic development. These findings may suggest that the temperature regulated pha-siRNAs could help to adapt the plants post embryonic development to changing temperature.

Furthermore, we identified temperature dependent 24-nt-long heterochromatic siRNA clusters at distinct sites which are usually associated with transposons. The number of transposon genes with significantly different siRNA production could be observed at higher temperature, especially in the flower and the seedling. In flowers, most of the transposons that were associated with significantly changed siRNA production belonged to the LTR/Gypsy superfamily, whereas in the seedling, almost every superfamily was represented.

The results of this research were continuously presented on international and national conferences, with 9 presentations (4 posters and 5 lectures). Preparation of a manuscript and a doctoral dissertation based on the results on the analysis of the role of small RNAs in temperature sensing in Arabidopsis is already in progress. The results and figures shown in this report outline the high quality of this study, which is anticipated to be published in a top academic peer reviewed journal with high impact factor. The results of this work are expected to be a highly cited reference for future studies.

Content:

1. Brief Introduction

Plants are sessile organisms, therefore it is vital to their survival to sense and readily adapt their growth and development in response to continuously changing environment. Temperature is a key environmental signal and accurate monitoring of ambient temperature is fundamental of living organisms. Plants measure temperature very accurately and can show remarkable responses to small changes in temperature (Argyris et al., 2005). For example, in response to higher temperatures plants grow faster and flower earlier, while plants grown in cold remain smaller and more compact. Some of these responses (like vernalization) accumulate data on temperature for several weeks; while others (like thermotolerance) are fast. Temperature can dramatically affect plant growth and development; however how temperature is sensed and integrated into development is largely unknown. The majority of research so far has focused on plant-temperature responses mostly associated with temperature stress condition (cold or heat stress) (Penfield, 2008) and mechanisms by which plants sense ambient growth temperature (or non-stress temperature) remained mostly unknown. In a forward genetic screen in Arabidopsis, Kumar and Wigge (2010) found that chromatin has an important role in the detection of changes in ambient temperature. They showed that nucleosomes containing the alternative histone H2A.Z are essential to perceiving ambient temperature correctly and this provides thermosensory information that is used to coordinate the ambient temperature transcriptome. Nucleosomes play an active role in controlling gene expression through modulating the ability of transcription factors to access their cis elements (Lam et al., 2008; Segal and Widom, 2009). H2A.Z -containing nucleosomes exhibit a much tighter wrapping of their DNA than canonical H2A nucleosomes. The occupancy of H2A.Z-containing nucleosomes decreases with temperature and therefore can modulate gene expression in a temperature-dependent manner. The same effect was observed in budding yeast, indicating that this is an evolutionary conserved mechanism in eukaryotes. (Kumar and Wigge, 2010).

Gene expression is highly regulated in living organisms to ensure proper development and adequate responses to environmental changes. Since gene expression is a multi-step process it can be regulated at several levels. Short non coding RNAs (sRNA) have been recognised as important gene expression regulators and they can act both transcriptionally and post-transcriptionally (Voinnet, 2009; Carthew and Sontheimer, 2009). The unexpectedly complex sRNA content of plant cells suggests that these molecules have an extensive regulatory role in gene expression. The function of these regulatory sRNAs is to give sequence specificity to effector complexes. This layer of gene regulation is known as RNA silencing.

The sRNAs are 21-24 nt long and they belong to two major classes: microRNA (miRNA) and short interfering RNA (siRNA). All sRNA are generated by an RNAse-III type enzyme called DICER-LIKE *(DCL)* from double stranded RNA (dsRNA) but dsRNA can be formed through different mechanisms. MiRNAs are generated from precursor RNA (pre-

miRNA) where single-stranded primary transcripts form a hairpin structure and are cleaved during a stepwise process in the cell nucleus by DCL1. The mature miRNA duplex is transported to the cytoplasm, where one of the miRNA strand is incorporated into Ago1 (an Argonaute protein) and the other strand is degraded. Plant miRNAs have near-perfect complementarity to their target sites and they bind to these sites to guide the cleavage of target mRNAs (Llave et al., 2002), although there are examples where the translation of the mRNA is suppressed without a cleavage (Aukerman and Sakai, 2003; Chen, 2004; Brodersen et al., 2008). MiRNAs are mainly 21 nt long and are important regulators of endogenous gene expression during development and environmental adaptation as it have been demonstrated by the pleiotropic developmental abnormalities seen in many miRNA biogenesis mutant.

The other big class of small RNAs based on their biogenesis is siRNAs. SiRNAs are produced from long dsRNA precursor. SiRNAs can be categorized into many different groups, however based on the origin of the dsRNA and the type of their targets the two most important are the followings:

(1) phased siRNAs (pha-siRNAs; they are also known as trans-acting siRNAs or ta-siRNAs) are 21 nt long and they belong to a special class of endogenous siRNAs. Pha-siRNAs require components of both the miRNA and siRNA pathways for their biogenesis. They are produced from long non-coding transcripts, which are converted into dsRNA by an RNA Dependent RNA Polymerase 6 (RDR6) (Peragine et al., 2004; Vazquez et al., 2004). This long dsRNA is then cleaved in a phased dicing reaction by DCL4 to generate 21 nt ta-siRNAs (Gasciolli et al., 2005; Xie et al., 2005; Yoshikawa et al., 2005). The phase of the dicing reaction is determined by the initial miRNA cleavage site. Ta-siRNAs target and regulate mRNAs in a similar way as miRNAs.

(2), the vast majority of endogenous siRNAs form a complex population of more than 100,000 different siRNA transcribed from thousands of loci (Kasschau et al., 2007; Mosher et al., 2008). The dsRNAs precursor are produced by RDR2 and cleaved by DCL3 to produce 24 nt siRNAs. The biogenesis of these heterochromatin siRNAs also requires an RNA polymerase IV (PolIV), which is unique to the plant kingdom and homologues to DNA-dependent RNA polymerase II (Zhang et al., 2007). A subset of these 24 nt cis-acting siRNA molecules are involved in stress responses, others target DNA and cause changes in chromatin structures. PolV is another plant specific RNA polymerase that generates nascent scaffolds transcripts that serves as a platform for complexes (likely through base-pairing between AGO4/siRNA complexes and scaffold RNA) to direct DNA methylation in Arabidopsis (Wierzbicki et al., 2009; Zhong et al., 2014).

sRNAs are not only important in endogenous gene regulation they also play role in plant defence against molecular parasites, including viruses (Ding and Voinnet, 2007). Environmental factors, especially temperature has strong influence on the outcome of plant-virus interactions. We showed previously that siRNA mediated plant defence against molecular parasites is temperature dependent (Szittya et al., 2003). At low ambient temperature (15 °C) the level of virus or transgene-derived siRNAs are dramatically reduced and as a consequence, this led to enhanced virus susceptibility or to a loss of gene silencing

mediated transgenic phenotypes. In contrast, RNA silencing is activated and the amount of siRNAs gradually increases with temperature rising. We also showed that in contrast to siRNA production, the accumulations of three selected miRNAs (miR157, miR169 and miR171) were not affected by temperature in Arabidopsis seedlings. In a more detailed miRNA expression study, Lee et. al., (2010) analysed the expression levels of the 120 unique Arabidopsis miRNA loci in response to ambient temperature changes (16 and 23 °C) by using miRNA microarray and miRNA northern hybridization analysis. They identified six ambient temperature-responsive miRNAs (miR156, miR163, miR169, miR172, miR398 and miR399) and proposed that some miRNAs are involved in the ambient temperature response in Arabidopsis.

Since we and others showed that low temperature inhibits RNA silencing mediated defence and some of the endogenous sRNAs show temperature dependent expression, we hypothesized that they likely have a role in temperature sensing and mediating physiological answer to different ambient temperature. Therefore we proposed to use genomic tools to globally identify expressional changes of sRNAs in response to ambient temperature at genomic level in the model plant *Arabidopsis thaliana*. The results written here are not published yet, therefore we give a detailed description of our results here.

2. Identification of small RNAs in *Nicotiana benthamiana*

As a preliminary research of this OTKA project, we prepared next generation sequencing data from *N. benthamiana* mRNAs, sRNAs and miRNA cleaved mRNA libraries (degradome library) to test our bioinformatic pipelines. *N. benthamiana* is a widely used model plant species for research on plant-pathogen interactions as well as other areas of plant science. It can be easily transformed or agro-infiltrated; therefore it is commonly used in studies requiring protein localization, interaction, or plant-based systems for protein expression and purification. We used a comprehensive molecular approach to detect and to experimentally validate *N. benthamiana* miRNAs and their target mRNAs from various tissues. We identified 40 conserved miRNA families and 18 novel microRNA candidates and validated their target mRNAs with a genomic scale approach. The accumulation of thirteen novel miRNAs was confirmed by Northern blot analysis. The conserved and novel miRNA targets were found to be involved in various biological processes including transcription, RNA binding, DNA modification, signal transduction, stress response and metabolic process. Among the novel miRNA's targets we found the mRNA of REPRESSOR OF SILENCING (ROS1). Regulation of ROS1 by a miRNA provides a new regulatory layer to reinforce transcriptional gene silencing by a post-transcriptional repression of ROS1 activity. The identified conserved and novel miRNAs along with their target mRNAs also provides a tissue specific atlas of known and new miRNA expression and their cleaved target mRNAs of *N. benthamiana*. Thus this study will serve as a valuable resource to the plant research community that will be beneficial well into the future. The above summarised results were published in BMC Genomics (Baksa et al., 2015).

3. Investigating the role of small regulatory RNAs in temperature sensing in *Arabidopsis thaliana*

Plant development is responsive to temperature; therefore plants can measure temperature very accurately and can distinguish differences of 1 ^{o}C. To profile changes in mRNA and sRNA expression, we have grown *A. thaliana* Col-0 plants at three different ambient temperatures (15, 21 or 27 °C; Figure 1).

Figure 1. Arabidopsis Col-0 plants were grown at three different ambient temperatures (15, 21, 27 ^{o}C).
Plant development is responsive to changes in the ambient temperature and they adjust their growth and development in response to temperature cues. At lower ambient temperature (15 ^{o}C) the plant grows more rosettes leaf and start to flower significantly later than at higher ambient temperature (27 ^{o}C).

Arabidopsis plants were grown either in soil (flower and leaf samples) or on half-strength Murashige and Skoog plates (seedling and root samples) under standard growth conditions at 15, 21 or 27 °C under long day condition. We collected total RNA samples from seedling, root, leaf and flower tissues, than prepared genomic scale libraries (mRNA, small RNA and degradome a.k.a. genome-wide 5' RACE) for further analysis. We used Illumina deep-sequencing platform followed by computational methods to identify, profile and describe conserved and non-conserved sRNAs during different ambient temperature conditions. Furthermore we also identified sRNA cleaved mRNAs through genomic-scale high-throughput Illumina sequencing.

Following Illumina sequencing, raw small RNA sequences in fastq format were processed and filtered with cutadapt 1.9.1 (Martin, 2011) set to trim Illumina small RNA adaptor (5'-TGGAATTCTCGGGTGCCAAGG-3'), keep sequences between 18-35 nt that contain residues with quality higher than 20. Untrimmed sequences (containing no or incomplete adaptor sequence) were discarded. Quality check of the libraries before and after processing was performed using FastQC 0.11.3 (Andrews, 2010). Processed reads were aligned to the Arabidopsis thaliana TAIR10 reference genome with butter 0.3.3 (Axtell, 2014) (utilising bowtie 1.1.1) allowing 1 mismatch (Table 1). For the manipulation of the alignment files samtools 0.1.19 and bamtools 2.3.0 were utilised. Summary statistics for different annotations were prepared by a custom made Linux shell script. Plots and heatmaps were generated using various R packages. To make the read counts in different libraries comparable we applied a normalisation method as suggested by McCormick et al. (McCormick et al., 2011). Highly abundant and variable sources like reads aligned to structural RNAs (rRNA, tRNA, snRNA, snoRNA) or organellar (mitochondrial and chloroplastic) genomes were excluded from the

calculation of the normalisation factor but were not discarded. These effective library sizes were scaled to 1 million reads (RPM).

	Unprocessed	Processed			Discarded	Mapped			Unmapped			Uniquely mapped			Multi-mapped		
	Redundant	Redundant	Non-Redundant	Complexity	Redundant	Redundant	Non-Redundant	Complexity	Redundant	Non-Redundant	Complexity	Redundant	Non-Redundant	Complexity	Redundant	Non-Redundant	Complexity
Flower 15°C 1	12 485 960	12 337 909	2 271 637	0.1841	148 051	11 780 542	2 048 106	0.1739	557 367	223 531	0.401	8 179 120	1 433 767	0.1753	3 601 422	614 339	0.1706
Flower 15°C 2	18 615 780	18 460 973	3 762 118	0.2038	154 807	17 885 672	3 479 259	0.1945	575 301	282 859	0.4917	11 936 930	2 488 906	0.2085	5 948 742	990 353	0.1665
Flower 21°C 1	6 968 436	6 906 932	1 259 756	0.1824	61 504	6 701 427	1 153 778	0.1722	205 505	105 978	0.5157	4 455 784	789 973	0.1773	2 245 643	363 805	0.162
Flower 21°C 2	18 552 004	18 269 387	3 265 487	0.1787	282 617	17 828 409	3 032 858	0.1701	440 978	232 629	0.5275	10 532 297	2 185 142	0.2075	7 296 112	847 716	0.1162
Flower 27°C 1	8 123 862	7 917 323	1 971 771	0.249	206 539	7 375 383	1 772 587	0.2403	541 940	199 184	0.3675	4 757 724	1 262 506	0.2654	2 617 659	510 081	0.1949
Flower 27°C 2	34 594 159	34 266 319	3 928 191	0.1146	327 840	33 311 310	3 570 296	0.1072	955 009	357 895	0.3748	22 062 251	2 518 401	0.1141	11 249 059	1 051 895	0.0935
Leaf 15°C 1	10 505 972	10 408 796	1 672 553	0.1607	97 176	10 040 602	1 520 817	0.1515	368 194	151 736	0.4121	4 016 928	949 686	0.2364	6 023 674	571 131	0.0948
Leaf 15°C 2	5 276 498	5 223 169	1 056 878	0.2023	53 329	5 041 460	961 419	0.1907	181 709	95 459	0.5253	1 946 041	577 556	0.2968	3 095 419	383 863	0.124
Leaf 21°C 1	7 708 673	7 533 325	1 169 755	0.1553	175 348	7 246 408	1 058 000	0.146	286 917	111 755	0.3895	3 042 142	657 962	0.2163	4 204 266	400 038	0.0952
Leaf 21°C 2	7 958 675	7 905 518	1 172 747	0.1483	53 157	7 645 337	1 061 560	0.1389	260 181	111 187	0.4273	3 166 313	658 291	0.2079	4 479 024	403 269	0.09
Leaf 27°C 1	6 843 983	6 659 885	905 180	0.1359	184 098	6 242 158	741 940	0.1189	417 727	163 240	0.3908	1 419 256	384 185	0.2707	4 822 902	357 755	0.0742
Leaf 27°C 2	11 929 921	11 637 253	1 009 109	0.0867	292 668	11 220 481	887 861	0.0791	416 772	121 248	0.2909	3 404 332	456 924	0.1342	7 816 149	430 937	0.0551
Root 15°C 1	20 315 025	19 946 757	2 856 967	0.1432	368 268	13 944 996	2 324 054	0.1667	6 001 761	532 913	0.0888	4 992 989	1 507 134	0.3019	8 952 007	816 920	0.0913
Root 15°C 2	6 820 233	6 707 358	834 649	0.1244	112 875	6 530 129	758 599	0.1162	177 229	76 050	0.4291	1 179 033	435 683	0.3695	5 351 096	322 916	0.0603
Root 21°C 1	9 446 414	9 239 179	1 853 810	0.2006	207 235	8 905 547	1 690 294	0.1898	333 632	163 516	0.4901	3 046 187	1 075 277	0.353	5 859 360	615 017	0.105
Root 21°C 2	15 766 766	15 590 045	2 232 756	0.1432	176 721	15 184 885	2 044 600	0.1346	405 160	188 156	0.4644	4 859 434	1 300 960	0.2677	10 325 451	743 640	0.072
Root 27°C 1	5 087 668	4 992 683	1 092 650	0.2189	94 985	4 790 325	993 731	0.2074	202 358	98 919	0.4888	1 637 296	628 293	0.3837	3 153 029	365 438	0.1159
Root 27°C 2	5 771 046	5 692 567	843 373	0.1482	78 479	5 422 656	751 857	0.1387	269 911	91 516	0.3391	1 290 558	447 298	0.3466	4 132 098	304 559	0.0737
Seedling 15°C 1	17 075 959	16 570 649	2 972 525	0.1794	505 310	16 043 611	2 750 014	0.1714	527 038	222 511	0.4222	6 403 763	1 808 103	0.2824	9 639 848	941 911	0.0977
Seedling 15°C 2	6 715 201	6 645 127	1 191 855	0.1794	70 074	6 462 770	1 106 591	0.1712	182 357	85 264	0.4676	1 753 342	683 891	0.39	4 709 428	422 700	0.0898
Seedling 21°C 1	9 635 717	9 430 150	1 651 892	0.1752	205 567	9 183 463	1 526 161	0.1662	246 687	125 731	0.5097	2 987 139	960 612	0.3216	6 196 324	565 549	0.0913
Seedling 21°C 2	16 361 460	16 232 849	2 653 586	0.1635	128 611	15 767 768	2 443 086	0.1549	465 081	210 500	0.4526	5 954 542	1 610 696	0.2705	9 813 226	832 390	0.0848
Seedling 27°C 1	16 091 400	15 857 400	3 024 057	0.1907	234 000	15 229 531	2 752 892	0.1808	627 869	271 165	0.4319	6 727 659	1 802 046	0.2679	8 501 872	950 846	0.1118
Seedling 27°C 2	10 065 907	9 971 869	1 841 018	0.1846	94 038	9 161 846	1 639 444	0.1789	810 023	201 574	0.2488	3 759 883	1 055 568	0.2807	5 401 963	583 876	0.1081

Table 1. High-throughput sequencing statistics of Arabidopsis sRNAs. Sequencing statistics of sRNA samples by tissue type and growing temperature with biological replicates. The complexity index was calculated as non-redundant divided by redundant read count. The higher the complexity index, the more diverse the mature sRNA population is.

De novo small RNA locus prediction was carried out using ShortStack 3.4 (Johnson et al., 2016). The co-ordinates of the loci were converted into a bed format and the loci were annotated with bedtools 2.17.0 (Quinlan and Hall, 2010) using its intersect command and TAIR10 annotations as reference (also converted to bed format). Filtering of the loci by ShortStack tags was carried out using a custom R script. Heterochromatic siRNA loci were defined as having a 'Dicercall' parameter of '24' (dominant size class), not having a 'PhaseScore' and flagged as not 'MIRNA'. Phased RNA producing loci were accepted when the 'Dicercall' and 'PhaseSize' parameters were '21' or '24', the 'PhaseScore' was at least '25', and were flagged as not 'MIRNA'. Genome browser tracks for every sequence size class were created by bedtools genomecov command. Alignments to the plus or minus strands were calculated separately and then were merged into a single track. RNA-seq analysis was performed following the Tuxedo protocol (tophat 2.0.13) (Trapnell et al., 2012). The resulting tables were analysed and filtered with Vennt {https://github.com/drpowell/vennt}. GO enrichment analysis on the filtered gene lists were performed with AgriGO server (Du et al., 2010).

To find out the effect of ambient temperature on sRNA expression on the genomic level we profiled the sRNA expression at the three different temperatures (15^0C, 21^0C and 27 ^{0}C) to identify differentially expressed sRNA loci at temperature dependent manner (Figure 2.). We identified *de novo* all sRNA loci that showed temperature dependent expressional changes and we grouped them based on their biogenesis, functions or annotations. We found that small RNAs are produced all over the Arabidopsis genome; however most of the small RNA producing loci are depleted from the coding part of the genome.

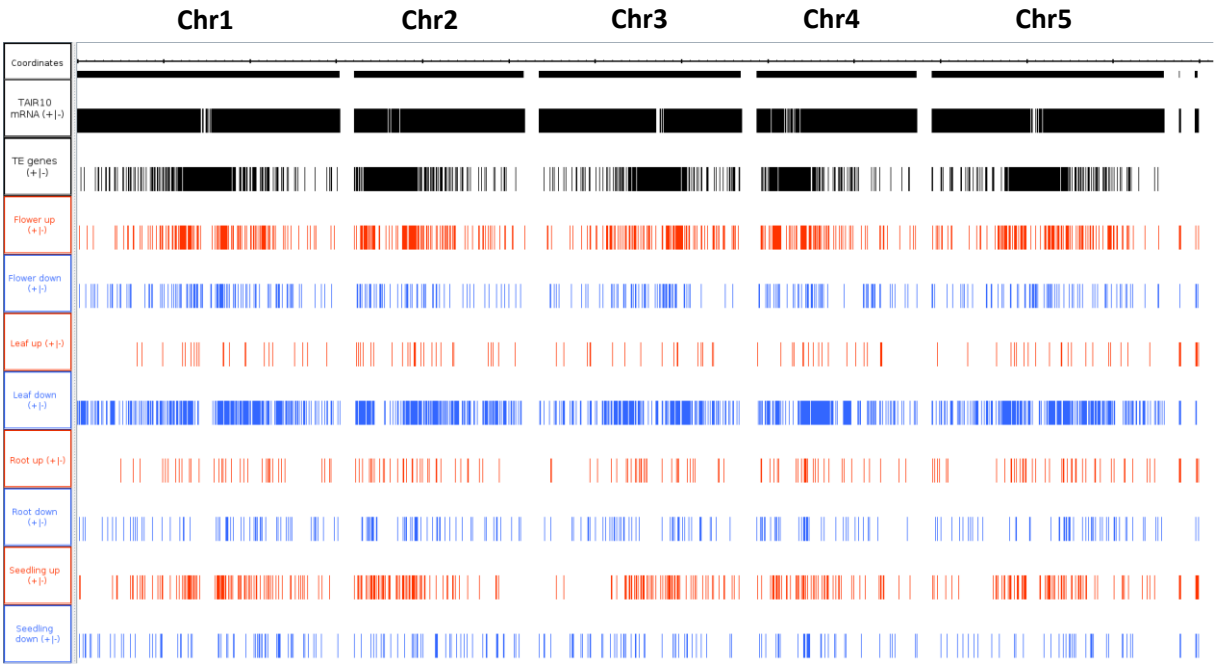

Figure 2. Genome browser tracks of the temperature regulated sRNA loci. The differential expression pattern of each temperature regulated sRNA loci can be directly compared between the different tissues or different temperatures using the prepared genome browser tracks. Each Arabidopsis chromosome is represented with a black horizontal line. The positions of mRNA coding genes and TE genes are represented as black vertical lines below each chromosome. The down regulated sRNA loci are represented as blue vertical lines and the up regulated sRNA loci are represented as red vertical lines in each tissue.

We grouped the small RNA producing loci based on the trend of the temperature dependent expressional pattern (increasing or decreasing trend). The resulting sRNA loci were further grouped based on their size or TAIR 10 functional annotations (miRNA, tasiRNA, siRNA, mRNA, snRNA, snoRNA, tRNA, rRNA, transposon, intergenic region etc.). Next we tested the GO term enrichment on those sRNA loci that were located in known protein coding genes. In the case of those sRNA loci that were located in transposons or intergenic regions we analysed the GO term enrichment of the nearest protein coding genes. During our analysis we found many sRNA loci with temperature dependent expression pattern and most of them were located in transposons or intergenic regions. Furthermore, we also found temperature dependent sRNA loci produced from tRNA genes (Figure 3). We tested two tRNA genes for sRNA production (tRNA fragments) with small RNA northern blots and we were able to confirm that these loci produced sRNAs in a temperature dependent fashion. Next we checked the biogenesis of these tRNA fragments (tRNA derived sRNAs) using dcl mutant *Arabidopsis* plants and we think that they are produced in a DCL2 dependent fashion (Figure 4). Although, the exact roles of tRNA fragments are yet to be elucidated, accumulating evidence suggests that tRNA-derived small RNAs participates translation regulation of gene expression under stress conditions. Furthermore, recent studies have demonstrated that tRNAs also serve as a major source of small non-coding RNAs that possess distinct and varied functions in both plants and animals. These tRNA fragments were shown to incorporate in AGO complexes and it is likely that they regulate gene expression post transcriptionally in a similar fashion as miRNAs do (Keam and Hutvagner 2015).

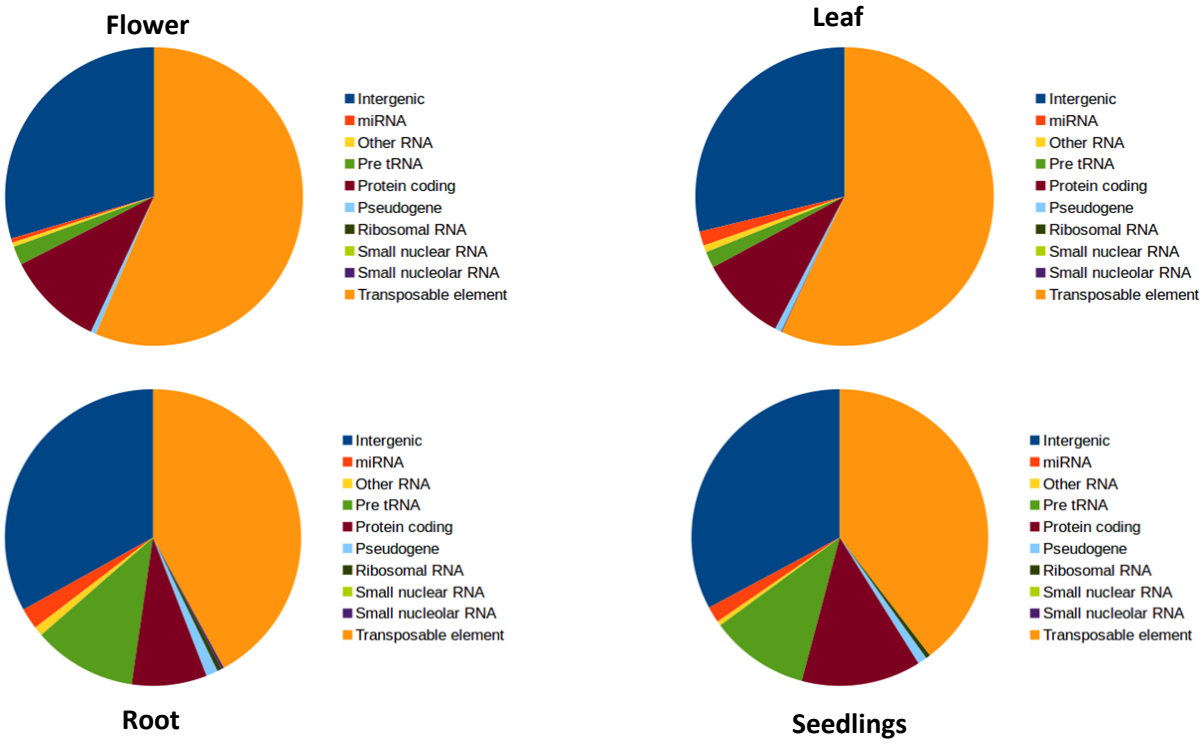

Figure 3. Pie chart of down regulated sRNA loci from four different tissues grouped by annotations.

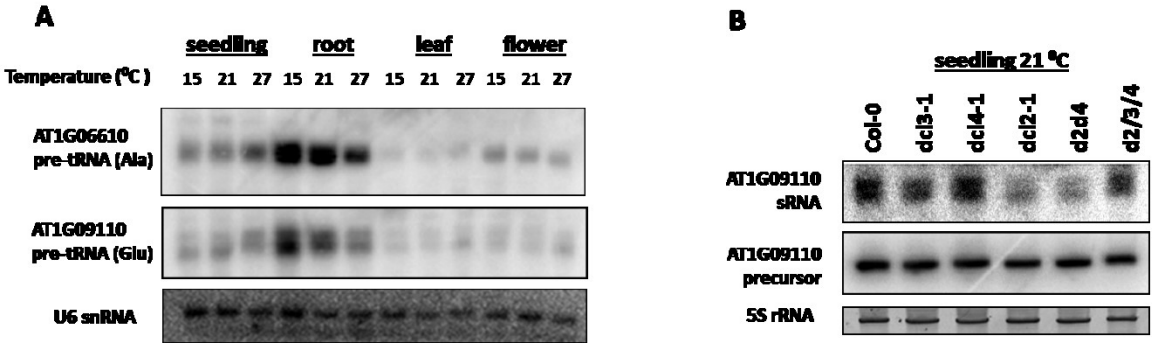

Figure 4. Temperature dependent expression of tRNA-derived sRNA fragments. A) Northern blot analysis of two tRNA genes for sRNA production in Arabidopsis wild type seedling, root, leaf and flower samples at three different temperatures. U6 snRNA represents a loading control here. B) tRNA fragments tested in dcl mutant (dcl3-1, dvl4-1, dcl2-1 d2d4 – dcl2-1/dcl4-1, d2/d3/d4 - dcl2-1/dcl3-1/dcl4-1) Arabidopsis seedlings grown at 21 0C. 5S rRNA is a loading control.

Among the sRNA loci that showed increasing expression trend with the elevation of ambient temperature (Figure 5.) the most interesting was the U12 minor spliceosome derived sRNAs. These sRNAs were derived from the 3' end of the U12 snRNA. It could be possible that U12 snRNA derived sRNAs might regulate U12 expression (Figure 6). U12 snRNA is a single copy gene in *Arabidopsis* and a component of the minor spliceosome. Regulation of U12 by temperature dependent sRNAs may lead to the regulation of genes that contain U12 dependent intron.

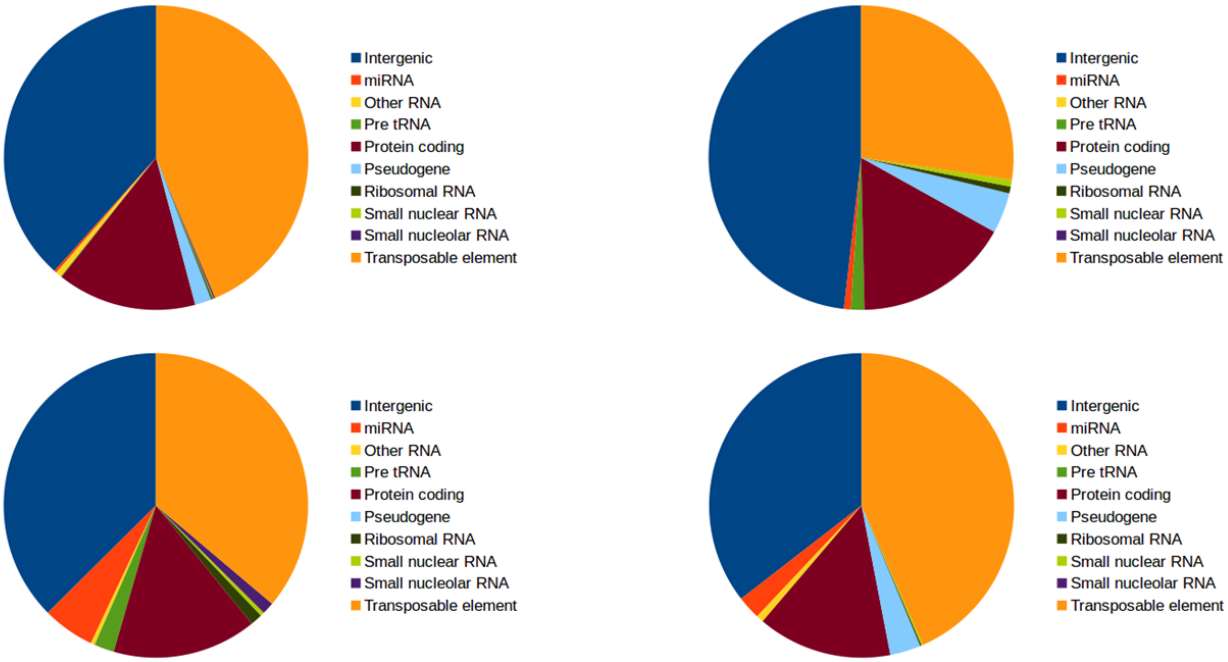

Figure 5. Pie chart of up regulated sRNA loci from four different tissues grouped by annotations.

A

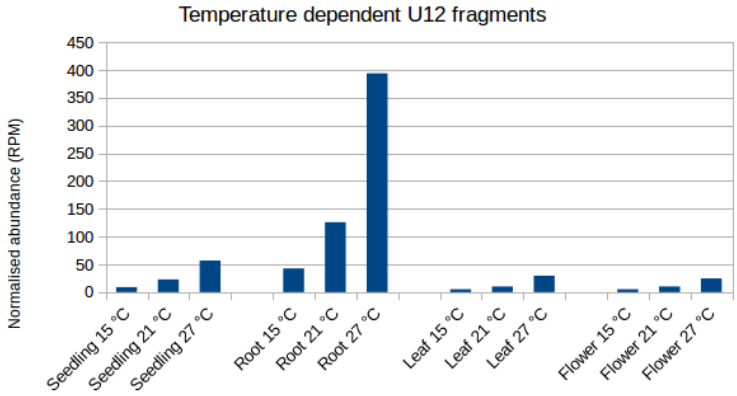

B

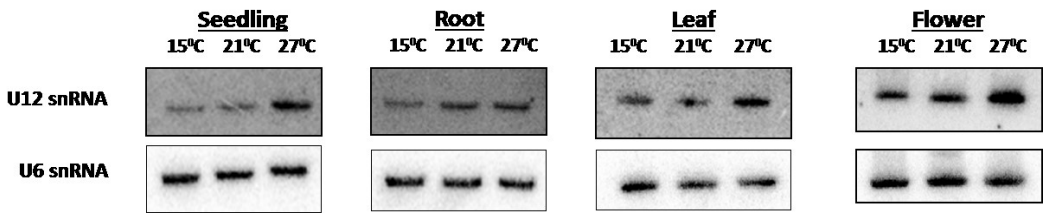

Figure 6. Temperature dependent expression of U12-derived sRNA fragments (A) and Northern blot validation of the temperature dependent expression pattern of U12 snRNA (B).

3.1. Identification of miRNAs and their target RNAs

Micro RNAs are the most characterised small RNA species in plants. They are processed from PolII-dependent self-complementary transcripts folding back to form hairpin structures. An RNaseII-like endonuclease, the Dicer-like 1 (DCL1) cleaves the hairpin out of the pri-miRNA sequence and then the same enzyme cuts the double stranded miRNA with 2nt 3' overhangs from a defined position. This duplex is then modified at the 2'-hydroxyl group at both 3' ends and loaded into the RISC complex containing Argonaute proteins. This enzyme cleaves one of the sequences in the duplex ("star" sequence), leaving the "mature" sequence bound that serves as a guide to cleave target mRNA sequences or in some cases, inhibits the translation of it. The maturation process has been extensively studied that led to the development of many bioinformatic tools that can predict miRNAs in plants with high confidence. We performed the *de novo* miRNA prediction with ShortStack 3.4 (Johnson et al., 2016) using all sRNA libraries. The sRNA clusters that qualified as miRNA were graphically represented (Figure 7).

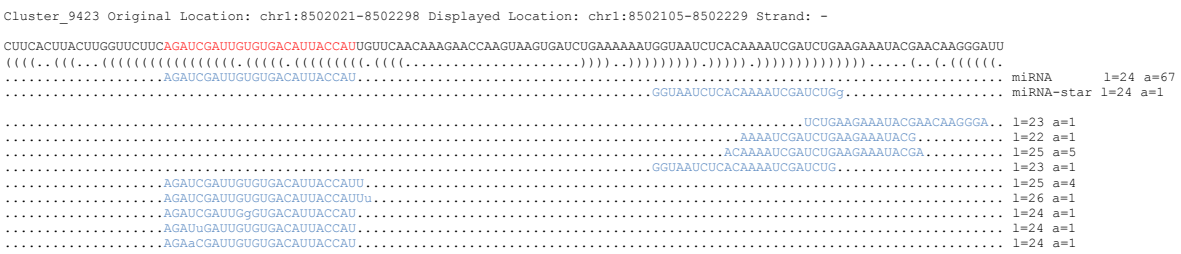

Figure 7. Graphical representation of a miRNA producing loci. The patterns of small RNA deep sequencing reads mapping to a newly identified microRNA in this projects. Hairpin microRNA sequences are shown at the top of the panel, with derived mature microRNA sequences shown in red, and predicted base-paired secondary structure in dot-bracket notation underneath. Read sequences are shown in blue, with the summed count across all data sets on the right. L represent the length of the sRNA sequence on the right.

Mature and star sequences (the most abundant sequence and the corresponding antiparallel sequence, respectively) were collected and compared to the nonredundant miRNA sequences deposited in miRBase v21. A union of the two sets were created and used for further analysis. Most of the *de novo* identified miRNA loci matched known miRNA genes but four potential novel miRNA loci have been identified as well. However, these newly identified miRNAs are hardly expressed under our conditions. However, they might be induced under other, more specific conditions like biotic or abiotic stresses or might be expressed in a few cells like in meristems or in tissues that we did not sample like seeds. Analysis of the hairpin structures of these novel miRNAs suggests that they are genuine miRNAs (Figure 8).

Cluster_9423 is located on chromosome 1 in the promoter of At1g24020, MLP-like protein 423 and produce 24-nt mature and star sequences. Cluster_27981 is also located on chromosome 1 in an intergenic region. This locus produces 23 and 21-nt long mature and star sequences, respectively. Despite its low abundance, we identified a category 0 target (At1g20570, Spc97) for the 23-nt-long mature sequence using our degradome libraries (Figure 9). Cluster_95379 is a mirtron that is located on chromosome 5 in the sixth intron of At5g17010, a Major Facilitator superfamily protein.

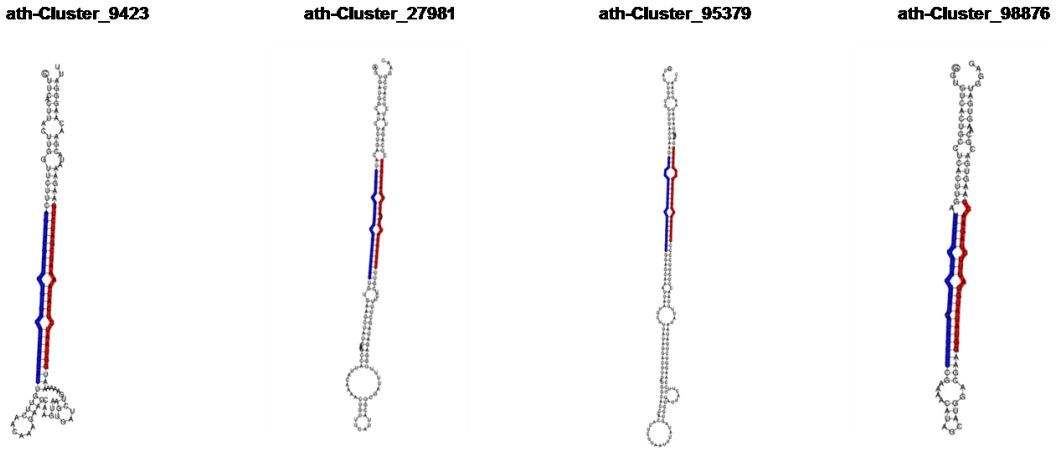

Figure 8. Secondary structures of the newly identified Arabidopsis miRNAs in our sRNA libraries. The mature miRNA and its star sequence are labelled as blue and red on the predicted secondary structure, respectively.

Both mature and star sequence is 21-nt-long. Cluster_98876 is also on chromosome 5 in an intergenic region. Its mature and star sequences are 22 and 21-nt-long, respectively. Both appear to be temperature dependent. However, because of its low abundance, these novel miRNAs were not considered in further analysis.

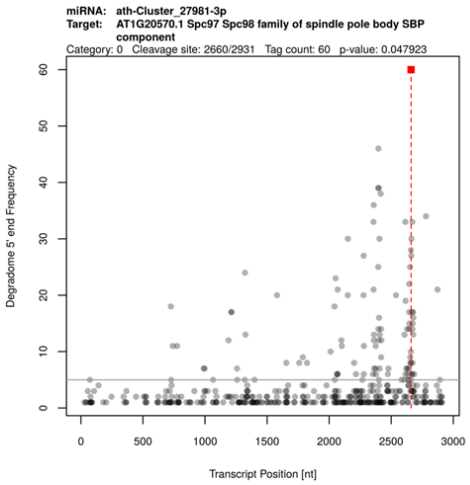

Figure 9. Target plots (t-plots) of Cluster_27981 miRNA target confirmed by degradome sequencing. In the head of the pictures there is a unique identifier of the mRNA followed by the annotation of the transcript. The relative degradome tag abundances are plotted against the nucleotide position within the transcript.

In our sRNA libraries we identified 28 miRNA families and 378 different miRNA sequences (not shown). Next we identified experimentally the target mRNAs of these miRNAs. To generate a miRNA cleaved target library (degradome) from Arabidopsis we applied a high-throghput experimental approach that can identify mRNAs targeted by sRNAs (German et al., 2009). The poly-A fraction of total RNA extracted from the different Arabidopsis tissues; seedling (Se), root (R), leaf (L), flower (F) were analysed for the identification of target transcripts of known and new miRNAs. We obtained a total number of 204 million short sequencing reads representing the 5' ends of uncapped, poly-adenylated RNAs. After initial processing, equal numbers of 20- and 21-nt sequence reads were obtained, and 90 % of the

SiteID	Query	Transcript	AllenScore	DegradomeCategory
AT1G01040-1_DCL1_CAF_SUS1_SIN1_ASU1_EMB76_EMB60_ATDCL1_dicer-like_1:3433	mir162b-3p	AT1G01040-1_DCL1_CAF_SUS1_SIN1_ASU1_EMB76_EMB60_ATDCL1_dicer-like_1	2	0
AT1G02860-1_NLA_BAH1_SPX_SYG1_Pho81_XPR1_domain-containing_protein:269	mir827a-3p	AT1G02860-1_NLA_BAH1_SPX_SYG1_Pho81_XPR1_domain-containing_protein	1	0
AT1G02860-2_NLA_SPX_SYG1_Pho81_XPR1_domain-containing_protein:269	mir827a-3p	AT1G02860-2_NLA_SPX_SYG1_Pho81_XPR1_domain-containing_protein	1	0
AT1G05630-1_AT5PTASE13_5PTASE13_Endonuclease_exonuclease_phosphatase_family_protein:2003	ath-mir164b-3p	AT1G05630-1_AT5PTASE13_5PTASE13_Endonuclease_exonuclease_phosphatase_family_protein	7,5	0
AT1G06580-1_Pentatricopeptide_repeat_PPR_superfamily_protein:875	mir161-5p	AT1G06580-1_Pentatricopeptide_repeat_PPR_superfamily_protein	3,5	0
AT1G07960-1_ATPDIL5-1_PDIL5-1_PDI-like_5-1:23	mir156h-5p	AT1G07960-1_ATPDIL5-1_PDIL5-1_PDI-like_5-1	8	0
AT1G08830-1_CSD1_copper_zinc_superoxide_dismutase_1:128	mir398b-3p	AT1G08830-1_CSD1_copper_zinc_superoxide_dismutase_1	5	0
AT1G08970-4_HAP5C_NF-YC9_nuclear_factor_Y_subunit_C9:611	ath-mir863-5p	AT1G08970-4_HAP5C_NF-YC9_nuclear_factor_Y_subunit_C9	8,5	0
AT1G09730-2_Cysteine_proteinases_superfamily_protein:1543	ath-mir826a	AT1G09730-2_Cysteine_proteinases_superfamily_protein	8	0
AT1G10120-1_basic_helix-loop-helix_bHLH_DNA-binding_superfamily_protein:1317	mir396b-5p	AT1G10120-1_basic_helix-loop-helix_bHLH_DNA-binding_superfamily_protein	5,5	0
AT1G10560-1_PUB18_ATPUB18_plant_U-box_18:1565	ath-mir870-3p	AT1G10560-1_PUB18_ATPUB18_plant_U-box_18	8,5	0
AT1G12520-3_ATCCS_CCS_copper_chaperone_for_SOD1:821	ath-mir398a-3p	AT1G12520-3_ATCCS_CCS_copper_chaperone_for_SOD1	6	0
AT1G12820-1_AFB3_auxin_signaling_F-box_3:1895	mir393a,b-5p	AT1G12820-1_AFB3_auxin_signaling_F-box_3	4	0
AT1G13600-1_AtbZIP58_bZIP58_basic_leucine-zipper_58:658	ath-mir829-5p	AT1G13600-1_AtbZIP58_bZIP58_basic_leucine-zipper_58	7,5	0
AT1G15125-1_S-adenosyl-L-methionine-dependent_methyltransferases_superfamily_protein:263	mir163-3p	AT1G15125-1_S-adenosyl-L-methionine-dependent_methyltransferases_superfamily_protein	6,5	0
AT1G17590-2_NF-YA8_nuclear_factor_Y_subunit_A8:1210	ath-mir169a-5p	AT1G17590-2_NF-YA8_nuclear_factor_Y_subunit_A8	3	0
AT1G17590-3_NF-YA8_nuclear_factor_Y_subunit_A8:1621	ath-mir169a-5p	AT1G17590-3_NF-YA8_nuclear_factor_Y_subunit_A8	3	0
AT1G20510-1_OPCL1_OPC-8_0_CoA_ligase1:1116	ath-mir841b-3p	AT1G20510-1_OPCL1_OPC-8_0_CoA_ligase1	7	0
AT1G20570-1_Spc97_Spc98_family_of_spindle_pole_body_SBP_component:2660	cluster_27981-3p	AT1G20570-1_Spc97_Spc98_family_of_spindle_pole_body_SBP_component	12,5	0
AT1G21410-1_SKP2A_F-box_RNI-like_superfamily_protein:1057	mir857a-3p	AT1G21410-1_SKP2A_F-box_RNI-like_superfamily_protein	11	0
AT1G21910-1_DREB26_Integrase-type_DNA-binding_superfamily_protein:371	ath-mir780.1	AT1G21910-1_DREB26_Integrase-type_DNA-binding_superfamily_protein	7	0
AT1G23580-1_Domain_of_unknown_function_DUF220:513	mir396b-5p	AT1G23580-1_Domain_of_unknown_function_DUF220	5	0
AT1G27360-1_SPL11_squamosa_promoter-like_11:1263	ath-mir156j	AT1G27360-1_SPL11_squamosa_promoter-like_11	0	0
AT1G27360-2_SPL11_squamosa_promoter-like_11:1223	ath-mir157d	AT1G27360-2_SPL11_squamosa_promoter-like_11	2	0
AT1G27360-4_SPL11_squamosa_promoter-like_11:1311	mir157d-5p	AT1G27360-4_SPL11_squamosa_promoter-like_11	3	0
AT1G27370-2_SPL10_squamosa_promoter_binding_protein-like_10:1457	mir157d-5p	AT1G27370-2_SPL10_squamosa_promoter_binding_protein-like_10	3	0
AT1G27370-4_SPL10_squamosa_promoter_binding_protein-like_10:1325	ath-mir156h	AT1G27370-4_SPL10_squamosa_promoter_binding_protein-like_10	2	0
AT1G30490-1_PHV_ATHB9_Homeobox-leucine_zipper_family_protein_lipid-binding_START_domain-containing_protein:806	mir165a,b-3p	AT1G30490-1_PHV_ATHB9_Homeobox-leucine_zipper_family_protein_lipid-binding_START_domain-containing_protein	3	0
AT1G31280-1_AGO2_Argonaute_family_protein:3233	mir403-3p	AT1G31280-1_AGO2_Argonaute_family_protein	1	0
AT1G34400-1_unknown_protein:342	ath-mir5013	AT1G34400-1_unknown_protein	7	0
AT1G48410-3_AGO1_Stabilizer_of_iron_transporter_SufD_Polynucleotidyl_transferase:532	mir168a,b-5p	AT1G48410-3_AGO1_Stabilizer_of_iron_transporter_SufD_Polynucleotidyl_transferase	5	0
AT1G48490-3_Protein_kinase_superfamily_protein:2937	mir396b-5p	AT1G48490-3_Protein_kinase_superfamily_protein	7	0
AT1G48500-2_JAZ4_TIFY6A_jasmonate-zim-domain_protein_4:975	mir169h,i,j,k,l,m,n-5p	AT1G48500-2_JAZ4_TIFY6A_jasmonate-zim-domain_protein_4	4	0
AT1G49910-1_BUB3.2_Transducin_WD40_repeat-like_superfamily_protein:1051	mir169e-3p	AT1G49910-1_BUB3.2_Transducin_WD40_repeat-like_superfamily_protein	4,5	0
AT1G49970-1_CLPR1_NCLPP5_SVR2_CLP_protease_proteolytic_subunit_1:1293	ath-mir5027	AT1G49970-1_CLPR1_NCLPP5_SVR2_CLP_protease_proteolytic_subunit_1	13,5	0
AT1G50055-1_TAS1B_TAS1B:374	ath-mir173-5p	AT1G50055-1_TAS1B_TAS1B	4,5	0
AT1G50670-1_OTU-like_cysteine_protease_family_protein:764	mir396b-5p	AT1G50670-1_OTU-like_cysteine_protease_family_protein	7	0
AT1G50930-1_unknown_protein:53	mir395a,e-3p	AT1G50930-1_unknown_protein	2	0
AT1G52150-1_ATHB-15_ATHB15_CNA_ICU4_Homeobox-leucine_zipper_family_protein_lipid-binding_START_domain-containing_protein:1279	mir166a,b,c,d,e,f,g-3p	AT1G52150-1_ATHB-15_ATHB15_CNA_ICU4_Homeobox-leucine_zipper_family_protein_lipid-binding_START_domain-containing_protein	3	0
AT1G52150-2_ATHB-15_ATHB15_CNA_ICU4_Homeobox-leucine_zipper_family_protein_lipid-binding_START_domain-containing_protein:1279	mir166a,b,c,d,e,f,g-3p	AT1G52150-2_ATHB-15_ATHB15_CNA_ICU4_Homeobox-leucine_zipper_family_protein_lipid-binding_START_domain-containing_protein	3	0
AT1G53160-1_SPL4_squamosa_promoter_binding_protein-like_4:602	ath-mir157d	AT1G53160-1_SPL4_squamosa_promoter_binding_protein-like_4	3	0
AT1G53230-1_TCP3_TEOSINTE_BRANCHED_1_cycloidea_and_PCF_transcription_factor_3:1195	ath-mir319c	AT1G53230-1_TCP3_TEOSINTE_BRANCHED_1_cycloidea_and_PCF_transcription_factor_3	3,5	0
AT1G53910-1_RAP2.12_related_to_AP2_12:598	mir396b-5p	AT1G53910-1_RAP2.12_related_to_AP2_12	6	0
AT1G54160-1_NFYA5_NF-YA5_nuclear_factor_Y_subunit_A5:1295	ath-mir169b,c-5p	AT1G54160-1_NFYA5_NF-YA5_nuclear_factor_Y_subunit_A5	3	0
AT1G56010-1_NAC1_anac021_NAC_domain_containing_protein_1:788	mir164a-5p	AT1G56010-1_NAC1_anac021_NAC_domain_containing_protein_1	2	0
AT1G56130-1_Leucine-rich_repeat_transmembrane_protein_kinase:348	mir390b-5p	AT1G56130-1_Leucine-rich_repeat_transmembrane_protein_kinase	5	0
AT1G57570-1_Mannose-binding_lectin_superfamily_protein:902	mir846a-3p	AT1G57570-1_Mannose-binding_lectin_superfamily_protein	3	0
AT1G60130-1_Mannose-binding_lectin_superfamily_protein:98	mir842a-3p	AT1G60130-1_Mannose-binding_lectin_superfamily_protein	2,5	0
AT1G62720-1_Pentatricopeptide_repeat_PPR-like_superfamily_protein:996	mir400-5p	AT1G62720-1_Pentatricopeptide_repeat_PPR-like_superfamily_protein	1	0
AT1G62910-1_Pentatricopeptide_repeat_PPR_superfamily_protein:997	ath-mir161.2	AT1G62910-1_Pentatricopeptide_repeat_PPR_superfamily_protein	3	0
AT1G64583-1_Tetratricopeptide_repeat_TPR_-like_superfamily_protein:739	mir161-5p	AT1G64583-1_Tetratricopeptide_repeat_TPR_-like_superfamily_protein	2,5	0
AT1G65340-1_CYP96A3_cytochrome_P450_family_96_subfamily_A_polypeptide_3:1266	ath-mir859	AT1G65340-1_CYP96A3_cytochrome_P450_family_96_subfamily_A_polypeptide_3	7,5	0
AT1G66690-1_S-adenosyl-L-methionine-dependent_methyltransferases_superfamily_protein:342	mir163-3p	AT1G66690-1_S-adenosyl-L-methionine-dependent_methyltransferases_superfamily_protein	1	0
AT1G66700-1_PXMT1_S-adenosyl-L-methionine-dependent_methyltransferases_superfamily_protein:358	mir163-3p	AT1G66700-1_PXMT1_S-adenosyl-L-methionine-dependent_methyltransferases_superfamily_protein	1	0
AT1G66700-3_PXMT1_S-adenosyl-L-methionine-dependent_methyltransferases_superfamily_protein:346	mir163-3p	AT1G66700-3_PXMT1_S-adenosyl-L-methionine-dependent_methyltransferases_superfamily_protein	1	0
AT1G66710-1_pseudogene_similar_to_AtPP_protein_blastp_match_of_55%_identity_and_1.0e-92_P-value_to_GP:490	mir163-3p	AT1G66710-1_pseudogene_similar_to_AtPP_protein_blastp_match_of_55%_identity_and_1.0e-92_P-value_to_GP	5	0
AT1G68580-2_agenet_domain-containing_protein_bromo-adjacent_homology_BAH_domain-containing_protein:1345	mir2111b-5p	AT1G68580-2_agenet_domain-containing_protein_bromo-adjacent_homology_BAH_domain-containing_protein	9	0
AT1G69040-1_ACR4_ACT_domain_repeat_4:573	mir393b-3p	AT1G69040-1_ACR4_ACT_domain_repeat_4	12	0
AT1G69170-1_Squamosa_promoter-binding_protein-like_SBP_domain_transcription_factor_family_protein:1307	mir156g-5p	AT1G69170-1_Squamosa_promoter-binding_protein-like_SBP_domain_transcription_factor_family_protein	2	0
AT1G69770-1_CMT3_chromomethylase_3:2037	mir823a-3p	AT1G69770-1_CMT3_chromomethylase_3	2,5	0
AT1G71360-1_Galactose-binding_protein:1941	mir156f-3p	AT1G71360-1_Galactose-binding_protein	6,5	0
AT1G72830-3_HAP2C_ATHAP2C_NF-YA3_nuclear_factor_Y_subunit_A3:1424	mir169h,i,j,k,l,m,n-5p	AT1G72830-3_HAP2C_ATHAP2C_NF-YA3_nuclear_factor_Y_subunit_A3	2,5	0
AT1G73300-1_scpl2_serine_carboxypeptidase-like_2:714	mir171b-5p	AT1G73300-1_scpl2_serine_carboxypeptidase-like_2	6,5	0
AT1G75190-1_unknown_protein:363	ath-mir865-3p	AT1G75190-1_unknown_protein	7,5	0
AT1G77850-1_ARF17_auxin_response_factor_17:1420	mir160b-5p	AT1G77850-1_ARF17_auxin_response_factor_17	0,5	0
AT1G80020-1_transposable_element_gene:3132	ath-mir159c	AT1G80020-1_transposable_element_gene	12	0
AT2G01990-1_unknown_protein:623	mir170,171a-5p	AT2G01990-1_unknown_protein	11	0
AT2G18540-1_RmlC-like_cupins_superfamily_protein:2008	mir156g-3p	AT2G18540-1_RmlC-like_cupins_superfamily_protein	5	0
AT2G22840-1_AtGRF1_GRF1_growth-regulating_factor_1:792	mir396b-5p	AT2G22840-1_AtGRF1_GRF1_growth-regulating_factor_1	4	0
AT2G27400-1_TAS1A_TAS1A:379	ath-mir173-5p	AT2G27400-1_TAS1A_TAS1A	2,5	0
AT2G27470-1_NF-YB11_nuclear_factor_Y_subunit_B11:841	mir156f-3p	AT2G27470-1_NF-YB11_nuclear_factor_Y_subunit_B11	5,5	0
AT2G28190-1_CSD2_CZSOD2_copper_zinc_superoxide_dismutase_2:487	mir398b-3p	AT2G28190-1_CSD2_CZSOD2_copper_zinc_superoxide_dismutase_2	7	0
AT2G28350-1_ARF10_auxin_response_factor_10:1340	mir160b-5p	AT2G28350-1_ARF10_auxin_response_factor_10	2	0
AT2G28550-3_RAP2.7_related_to_AP2.7:1613	mir172a,b-3p	AT2G28550-3_RAP2.7_related_to_AP2.7	3	0
AT2G29130-1_LAC2_ATLAC2_laccase_2:740	ath-mir397a	AT2G29130-1_LAC2_ATLAC2_laccase_2	1,5	0
AT2G32700-2_LUH_LEUNIG_homolog:2453	mir396b-5p	AT2G32700-2_LUH_LEUNIG_homolog	13,5	0
AT2G33790-1_ATAGP30_AGP30_arabinogalactan_protein_30:473	ath-mir838	AT2G33790-1_ATAGP30_AGP30_arabinogalactan_protein_30	7	0
AT2G33810-1_SPL3_squamosa_promoter_binding_protein-like_3:797	mir156g-5p	AT2G33810-1_SPL3_squamosa_promoter_binding_protein-like_3	2,5	0
AT2G34010-1_unknown_protein:449	ath-mir159a	AT2G34010-1_unknown_protein	3	0
AT2G34710-1_PHB_ATHB14_ATHB-14_PHB-1D_Homeobox-leucine_zipper_family_protein_lipid-binding_START_domain-containing_protein:881	mir165a,b-3p	AT2G34710-1_PHB_ATHB14_ATHB-14_PHB-1D_Homeobox-leucine_zipper_family_protein_lipid-binding_START_domain-containing_protein	3	0
AT2G36145-1_unknown_protein:564	mir396b-5p	AT2G36145-1_unknown_protein	6	0
AT2G36400-1_AtGRF3_GRF3_growth-regulating_factor_3:757	mir396b-5p	AT2G36400-1_AtGRF3_GRF3_growth-regulating_factor_3	4	0
AT2G39250-1_SNZ_Integrase-type_DNA-binding_superfamily_protein:1055	ath-mir172e-3p	AT2G39250-1_SNZ_Integrase-type_DNA-binding_superfamily_protein	2,5	0
AT2G39675-1_TAS1C_TAS1C:379	ath-mir173-5p	AT2G39675-1_TAS1C_TAS1C	2,5	0
AT2G39681-1_TAS2_TAS2:418	ath-mir173-5p	AT2G39681-1_TAS2_TAS2	2,5	0
AT2G41710-2_Integrase-type_DNA-binding_superfamily_protein:1217	mir8170-3p	AT2G41710-2_Integrase-type_DNA-binding_superfamily_protein	9,5	0
AT2G42200-1_SPL9_AtSPL9_squamosa_promoter_binding_protein-like_9:948	mir156h-5p	AT2G42200-1_SPL9_AtSPL9_squamosa_promoter_binding_protein-like_9	2	0
AT2G42510-1_FUNCTIONS_IN_molecular_function_unknown:1485	mir398a-5p	AT2G42510-1_FUNCTIONS_IN_molecular_function_unknown	12,5	0
AT2G45160-1_HAM1_ATHAM1_LOM1_GRAS_family_transcription_factor:1014	mir171a-3p	AT2G45160-1_HAM1_ATHAM1_LOM1_GRAS_family_transcription_factor	0	0
AT2G45480-1_AtGRF9_GRF9_growth-regulating_factor_9:525	mir396b-5p	AT2G45480-1_AtGRF9_GRF9_growth-regulating_factor_9	4	0
AT2G47460-1_MYB12_ATMYB12_PFG1_myb_domain_protein_12:401	ath-mir858b	AT2G47460-1_MYB12_ATMYB12_PFG1_myb_domain_protein_12	2,5	0
AT3G03030-1_F-box_RNI-like_superfamily_protein:1260	ath-mir5016	AT3G03030-1_F-box_RNI-like_superfamily_protein	14,5	0
AT3G03726-1_Protein_of_unknown_function_DUF295:716	mir5650-3p	AT3G03726-1_Protein_of_unknown_function_DUF295	8	0
AT3G05650-1_AtRLP32_RLP32_receptor_like_protein_32:2303	ath-mir5016	AT3G05650-1_AtRLP32_RLP32_receptor_like_protein_32	7	0
AT3G05690-1_UNE8_ATHAP2B_HAP2B_NF-YA2_nuclear_factor_Y_subunit_A2:1194	mir169h,i,j,k,l,m,n-5p	AT3G05690-1_UNE8_ATHAP2B_HAP2B_NF-YA2_nuclear_factor_Y_subunit_A2	3	0
AT3G11440-1_ATMYB65_MYB65_myb_domain_protein_65:1166	ath-mir159a	AT3G11440-1_ATMYB65_MYB65_myb_domain_protein_65	3,5	0
AT3G12977-1_NAC_No_Apical_Meristem_domain_transcriptional_regulator_superfamily_protein:728	mir164a-5p	AT3G12977-1_NAC_No_Apical_Meristem_domain_transcriptional_regulator_superfamily_protein	2,5	0
AT3G14110-1_FLU_Tetratricopeptide_repeat_TPR_-like_superfamily_protein:740	mir396b-5p	AT3G14110-1_FLU_Tetratricopeptide_repeat_TPR_-like_superfamily_protein	4,5	0
AT3G15030-1_TCP4_MEE35_TCP_family_transcription_factor_4:1487	ath-mir319c	AT3G15030-1_TCP4_MEE35_TCP_family_transcription_factor_4	3	0
AT3G15170-1_CUC1_ANAC054_ATNAC1_NAC_No_Apical_Meristem_domain_transcriptional_regulator_superfamily_protein:675	mir164a-5p	AT3G15170-1_CUC1_ANAC054_ATNAC1_NAC_No_Apical_Meristem_domain_transcriptional_regulator_superfamily_protein	2,5	0
AT3G15270-1_SPL5_squamosa_promoter_binding_protein-like_5:655	ath-mir156j	AT3G15270-1_SPL5_squamosa_promoter_binding_protein-like_5	2	0
AT3G15770-2_unknown_protein:508	ath-mir5642a,b	AT3G15770-2_unknown_protein	12,5	0
AT3G16710-1_Pentatricopeptide_repeat_PPR_superfamily_protein:996	mir400-5p	AT3G16710-1_Pentatricopeptide_repeat_PPR_superfamily_protein	2,5	0
AT3G17140-1_Plant_invertase_pectin_methylesterase_inhibitor_superfamily_protein:62	ath-mir858b	AT3G17140-1_Plant_invertase_pectin_methylesterase_inhibitor_superfamily_protein	7	0
AT3G17715-1_pseudogene_similar_to_S-adenosylmethionine_decarboxylase_proenzyme_3_EC_4.1.1.50_AdoMetDC_3_SamDC_3_Contains_S-ad	mir850a-3p	AT3G17715-1_pseudogene_similar_to_S-adenosylmethionine_decarboxylase_proenzyme_3_EC_4.1.1.50_AdoMetDC_3_SamDC_3_Contains_S-ader	10	0
AT3G21300-1_RNA_methyltransferase_family_protein:1249	mir156g-5p	AT3G21300-1_RNA_methyltransferase_family_protein	4,5	0
AT3G22890-1_APS1_ATP_sulfurylase_1:453	mir395a,e-3p	AT3G22890-1_APS1_ATP_sulfurylase_1	3,5	0
AT3G26810-1_AFB2_auxin_signaling_F-box_2:2010	ath-mir393a,b-5p	AT3G26810-1_AFB2_auxin_signaling_F-box_2	4	0
AT3G27150-1_Galactose_oxidase_kelch_repeat_superfamily_protein:301	mir2111b-5p	AT3G27150-1_Galactose_oxidase_kelch_repeat_superfamily_protein	2	0
AT3G27200-1_Cupredoxin_superfamily_protein:269	ath-mir398a-3p	AT3G27200-1_Cupredoxin_superfamily_protein	5,5	0
AT3G28460-1_methyltransferases:61	mir173-5p	AT3G28460-1_methyltransferases	5	0
AT3G44860-1_FAMT_farnesoic_acid_carboxyl-O-methyltransferase:331	mir163-3p	AT3G44860-1_FAMT_farnesoic_acid_carboxyl-O-methyltransferase	3	0
AT3G51140-1_Protein_of_unknown_function_DUF3353:993	ath-mir781a,b	AT3G51140-1_Protein_of_unknown_function_DUF3353	10	0
AT3G51760-1_Protein_of_unknown_function_DUF688:783	ath-mir829-3p.2	AT3G51760-1_Protein_of_unknown_function_DUF688	18	0
AT3G51780-1_ATBAG4_BAG4_BCL-2-associated_athanogene_4:827	ath-mir5998a,b	AT3G51780-1_ATBAG4_BAG4_BCL-2-associated_athanogene_4	9	0
AT3G52910-1_AtGRF4_GRF4_growth-regulating_factor_4:753	mir396a-5p	AT3G52910-1_AtGRF4_GRF4_growth-regulating_factor_4	4	0
AT3G54630-1_CONTAINS_InterPro_DOMAIN_s_Kinetochore_protein_Ndc80_InterPro_IPR005550_:1083	mir156g-3p	AT3G54630-1_CONTAINS_InterPro_DOMAIN_s_Kinetochore_protein_Ndc80_InterPro_IPR005550_	9,5	0
AT3G54990-1_SMZ_Integrase-type_DNA-binding_superfamily_protein:976	ath-mir172e-3p	AT3G54990-1_SMZ_Integrase-type_DNA-binding_superfamily_protein	2	0
AT3G57230-1_AGL16_AGAMOUS-like_16:796	ath-mir824-5p	AT3G57230-1_AGL16_AGAMOUS-like_16	0,5	0
AT3G57230-2_AGL16_AGAMOUS-like_16:597	ath-mir824-5p	AT3G57230-2_AGL16_AGAMOUS-like_16	0,5	0
AT3G57920-1_SPL15_squamosa_promoter_binding_protein-like_15:856	mir156h-5p	AT3G57920-1_SPL15_squamosa_promoter_binding_protein-like_15	2	0
AT3G58110-1_unknown_protein:226	ath-mir831-3p	AT3G58110-1_unknown_protein	12	0
AT3G59765-1_other_RNA:166	ath-mir5027	AT3G59765-1_other_RNA	7,5	0
AT3G60250-2_CKB3_casein_kinase_II_beta_chain_3:243	mir397b-5p	AT3G60250-2_CKB3_casein_kinase_II_beta_chain_3	4	0
AT3G60630-1_HAM2_ATHAM2_LOM2_GRAS_family_transcription_factor:1053	mir171b,c-3p	AT3G60630-1_HAM2_ATHAM2_LOM2_GRAS_family_transcription_factor	4	0
AT3G61250-1_AtMYB17_MYB17_myb_domain_protein_17:604	ath-mir858b	AT3G61250-1_AtMYB17_MYB17_myb_domain_protein_17	5	0
AT3G62980-1_TIR1_F-box_RNI-like_superfamily_protein:1722	ath-mir393a,b-5p	AT3G62980-1_TIR1_F-box_RNI-like_superfamily_protein	2	0
AT3G66658-2_ALDH22A1_aldehyde_dehydrogenase_22A1:1112	ath-mir319c	AT3G66658-2_ALDH22A1_aldehyde_dehydrogenase_22A1	3	0
AT4G00150-1_HAM3_ATHAM3_LOM3_GRAS_family_transcription_factor:867	mir170-3p	AT4G00150-1_HAM3_ATHAM3_LOM3_GRAS_family_transcription_factor	1,5	0
AT4G03190-1_GRH1_ATGRH1_AFB1_GRR1-like_protein_1:1598	mir393a,b-5p	AT4G03190-1_GRH1_ATGRH1_AFB1_GRR1-like_protein_1	2	0
AT4G04780-1_MED21_mediator_21:132	ath-mir161.2	AT4G04780-1_MED21_mediator_21	7,5	0
AT4G06720-1_transposable_element_gene:1806	mir398b-3p	AT4G06720-1_transposable_element_gene	6	0
AT4G13450-2_Adenine_nucleotide_alpha_hydrolases-like_superfamily_protein:734	mir158b-5p	AT4G13450-2_Adenine_nucleotide_alpha_hydrolases-like_superfamily_protein	6,5	0
AT4G18260-1_Cytochrome_b561_ferric_reductase_transmembrane_protein_family:1057	mir156g-3p	AT4G18260-1_Cytochrome_b561_ferric_reductase_transmembrane_protein_family	5	0
AT4G19440-1_Tetratricopeptide_repeat_TPR_-like_superfamily_protein:1249	mir400-5p	AT4G19440-1_Tetratricopeptide_repeat_TPR_-like_superfamily_protein	2	0
AT4G23010-1_ATUTR2_UTR2_UDP-galactose_transporter_2:1002	mir164a-3p	AT4G23010-1_ATUTR2_UTR2_UDP-galactose_transporter_2	12,5	0
AT4G23120-1_Bromo-adjacent_homology_BAH_domain-containing_protein:1054	mir158b-5p	AT4G23120-1_Bromo-adjacent_homology_BAH_domain-containing_protein	10	0
AT4G24150-1_AtGRF8_GRF8_growth-regulating_factor_8:848	mir396b-5p	AT4G24150-1_AtGRF8_GRF8_growth-regulating_factor_8	4	0
AT4G26570-1_ATCBL3_CBL3_calcineurin_B-like_3:672	ath-mir868-5p	AT4G26570-1_ATCBL3_CBL3_calcineurin_B-like_3	18,5	0
AT4G26582-1_Potential_natural_antisense_gene_locus_overlaps_with_AT4G26590:343	ath-mir780.1	AT4G26582-1_Potential_natural_antisense_gene_locus_overlaps_with_AT4G26590	5,5	0
AT4G26930-1_MYB97_AtMYB97_myb_domain_protein_97:321	ath-mir858b	AT4G26930-1_MYB97_AtMYB97_myb_domain_protein_97	6	0
AT4G27090-1_Ribosomal_protein_L14:400	ath-mir167c-5p	AT4G27090-1_Ribosomal_protein_L14	28	0
AT4G30080-1_ARF16_auxin_response_factor_16:1519	mir160b-5p	AT4G30080-1_ARF16_auxin_response_factor_16	2,5	0
AT4G31120-1_SKB1_ATPRMT5_SHK1_binding_protein_1:610	mir396b-5p	AT4G31120-1_SKB1_ATPRMT5_SHK1_binding_protein_1	7	0
AT4G32880-1_ATHB-8_ATHB8_HB-8_homeobox_gene_8:945	mir165a,b-3p	AT4G32880-1_ATHB-8_ATHB8_HB-8_homeobox_gene_8	3	0
AT4G36920-1_AP2_FLO2_FL1_Integrase-type_DNA-binding_superfamily_protein:1340	mir172c,d-3p	AT4G36920-1_AP2_FLO2_FL1_Integrase-type_DNA-binding_superfamily_protein	1	0
AT4G37740-1_AtGRF2_GRF2_growth-regulating_factor_2:921	mir396b-5p	AT4G37740-1_AtGRF2_GRF2_growth-regulating_factor_2	4	0
AT5G04210-1_CCCH-type_zinc_fingerfamily_protein_with_RNA-binding_domain:117	ath-mir863-5p	AT5G04210-1_CCCH-type_zinc_fingerfamily_protein_with_RNA-binding_domain	12	0
AT5G04950-1_NAS1_ATNAS1_nicotianamine_synthase_1:892	ath-mir2111a-3p	AT5G04950-1_NAS1_ATNAS1_nicotianamine_synthase_1	17	0
AT5G05450-1_P-loop_containing_nucleoside_triphosphate_hydrolases_superfamily_protein:1244	ath-mir5637	AT5G05450-1_P-loop_containing_nucleoside_triphosphate_hydrolases_superfamily_protein	14,5	0
AT5G06510-1_NF-YA10_nuclear_factor_Y_subunit_A10:1078	mir169h,i,j,k,l,m,n-5p	AT5G06510-1_NF-YA10_nuclear_factor_Y_subunit_A10	3	0
AT5G07680-2_ANAC080_NAC080_NAC_domain_containing_protein_80:662	mir164c-5p	AT5G07680-2_ANAC080_NAC080_NAC_domain_containing_protein_80	2,5	0
AT5G08380-1_AtAGAL1_AGAL1_alpha-galactosidase_1:677	ath-mir781a,b	AT5G08380-1_AtAGAL1_AGAL1_alpha-galactosidase_1	15,5	0
AT5G09670-1_loricrin-related:2493	mir773a-3p	AT5G09670-1_loricrin-related	6,5	0
AT5G12840-4_HAP2A_ATHAP2A_NF-YA1_nuclear_factor_Y_subunit_A1:1130	ath-mir169b,c-5p	AT5G12840-4_HAP2A_ATHAP2A_NF-YA1_nuclear_factor_Y_subunit_A1	3	0
AT5G16730-1_Plant_protein_of_unknown_function_DUF827:2098	mir773a-3p	AT5G16730-1_Plant_protein_of_unknown_function_DUF827	6,5	0
AT5G17030-1_UGT78D3_UDP-glucosyl_transferase_78D3:1099	ath-mir390b-3p	AT5G17030-1_UGT78D3_UDP-glucosyl_transferase_78D3	7	0
AT5G17530-3_phosphoglucosamine_mutase_family_protein:1218	mir859a-3p	AT5G17530-3_phosphoglucosamine_mutase_family_protein	8	0
AT5G18065-1_unknown_protein:656	ath-mir319a,b	AT5G18065-1_unknown_protein	15	0
AT5G20230-1_ATBCB_BCB_SAG14_blue-copper-binding_protein:98	ath-mir398a-3p	AT5G20230-1_ATBCB_BCB_SAG14_blue-copper-binding_protein	12,5	0
AT5G23790-1_AtGolS5_GolS5_galactinol_synthase_5:832	ath-mir863-5p	AT5G23790-1_AtGolS5_GolS5_galactinol_synthase_5	7,5	0
AT5G38100-1_S-adenosyl-L-methionine-dependent_methyltransferases_superfamily_protein:328	mir163-3p	AT5G38100-1_S-adenosyl-L-methionine-dependent_methyltransferases_superfamily_protein	6,5	0
AT5G38550-1_Mannose-binding_lectin_superfamily_protein:176	mir842a-3p	AT5G38550-1_Mannose-binding_lectin_superfamily_protein	2,5	0
AT5G39610-1_ATNAC2_ORE1_ANAC092_ATNAC6_NAC2_NAC6_NAC_domain_containing_protein_6:781	mir164c-5p	AT5G39610-1_ATNAC2_ORE1_ANAC092_ATNAC6_NAC2_NAC6_NAC_domain_containing_protein_6	3	0
AT5G41170-1_Pentatricopeptide_repeat_PPR-like_superfamily_protein:892	ath-mir161.2	AT5G41170-1_Pentatricopeptide_repeat_PPR-like_superfamily_protein	3	0
AT5G41540-1_Disease_resistance_protein_TIR-NBS-LRR_class_family:1546	mir393b-3p	AT5G41540-1_Disease_resistance_protein_TIR-NBS-LRR_class_family	7,5	0
AT5G43740-1_Disease_resistance_protein_CC-NBS-LRR_class_family:617	ath-mir472-3p	AT5G43740-1_Disease_resistance_protein_CC-NBS-LRR_class_family	1	0
AT5G43740-2_Disease_resistance_protein_CC-NBS-LRR_class_family:643	ath-mir472-3p	AT5G43740-2_Disease_resistance_protein_CC-NBS-LRR_class_family	1	0
AT5G44290-2_Protein_kinase_superfamily_protein:1305	mir165b-5p	AT5G44290-2_Protein_kinase_superfamily_protein	11	0
AT5G49850-1_Mannose-binding_lectin_superfamily_protein:799	mir846a-3p	AT5G49850-1_Mannose-binding_lectin_superfamily_protein	3	0
AT5G50570-2_SPL13A_SPL13_Squamosa_promoter-binding_protein-like_SBP_domain_transcription_factor_family_protein:977	ath-mir156j	AT5G50570-2_SPL13A_SPL13_Squamosa_promoter-binding_protein-like_SBP_domain_transcription_factor_family_protein	0	0
AT5G50670-1_SPL13B_SPL13_Squamosa_promoter-binding_protein-like_SBP_domain_transcription_factor_family_protein:1112	ath-mir156j	AT5G50670-1_SPL13B_SPL13_Squamosa_promoter-binding_protein-like_SBP_domain_transcription_factor_family_protein	0	0
AT5G51660-1_CPSF160_ATCPSF160_cleavage_and_polyadenylation_specificity_factor_160:3367	ath-mir5998a,b	AT5G51660-1_CPSF160_ATCPSF160_cleavage_and_polyadenylation_specificity_factor_160	8,5	0
AT5G52600-1_AtMYB82_MYB82_myb_domain_protein_82:334	ath-mir828	AT5G52600-1_AtMYB82_MYB82_myb_domain_protein_82	3	0
AT5G53950-1_CUC2_ANAC098_ATCUC2_NAC_No_Apical_Meristem_domain_transcriptional_regulator_superfamily_protein:812	mir164a-5p	AT5G53950-1_CUC2_ANAC098_ATCUC2_NAC_No_Apical_Meristem_domain_transcriptional_regulator_superfamily_protein	2,5	0
AT5G57735-1_TASIR-ARF_tasiR-ARF:429	mir390b-5p	AT5G57735-1_TASIR-ARF_tasiR-ARF	4,5	0
AT5G60120-1_TOE2_target_of_early_activation_tagged_EAT_2:1658	mir172a,b-3p	AT5G60120-1_TOE2_target_of_early_activation_tagged_EAT_2	1	0
AT5G60690-1_REV_IFL_IFL1_Homeobox-leucine_zipper_family_protein_lipid-binding_START_domain-containing_protein:1273	mir165a,b-3p	AT5G60690-1_REV_IFL_IFL1_Homeobox-leucine_zipper_family_protein_lipid-binding_START_domain-containing_protein	3	0
AT5G64770-1_RGF9_Encodes_a_root_meristem_growth_factor_RGF_._Belongs_to_a_family_of_functionally_redundant_homologous_peptides_that	ath-mir830-3p	AT5G64770-1_RGF9_Encodes_a_root_meristem_growth_factor_RGF_._Belongs_to_a_family_of_functionally_redundant_homologous_peptides_that_	17	0
AT5G66420-2_LOCATED_IN_cellular_component_unknown:1637	mir396b-5p	AT5G66420-2_LOCATED_IN_cellular_component_unknown	5	0
AT5G67180-1_TOE3_target_of_early_activation_tagged_EAT_3:1309	mir172a,b-3p	AT5G67180-1_TOE3_target_of_early_activation_tagged_EAT_3	3	0

Table 2. Category 0 targets of Arabidopsis miRNAs.

short sequencing reads could be mapped to the Arabidopsis transcriptome. In plants, miRNA mediated mRNA cleavage is highly specific and miRNAs have been shown to bind with near perfect complementarity to their mRNA targets, that generally leading to the slicing of the

mRNA between positions 10 and 11 of the AGO1 bound miRNA. As a consequence, the cleaved mRNA targets should have distinct peaks in the degradome sequence tags at the predicted cleavage site relative to the other regions of the transcript. In our analysis we have applied the CleaveLand4 pipeline (Brousse et al., 2014) to identify cleaved targets for both known and new miRNAs. Abundance of the sequenced tags was plotted on each transcript and the cleaved target transcripts have been categorized into five classes (categories 0, 1, 2, 3 and 4) as it was defined previously in CleaveLand (version2) (Addo-Quaye et al., 2009). In our target list we kept high-confidence miRNA-target gene interactions (categories 0, 1, 2) and only category 3 targets as low–confidence miRNA-target pairs. Category 4 targets are defined as only one raw read at the expected cleavage position, however it might also be the result of the degradation of the target RNA, therefore they were omitted from our target list. We identified 187 miRNA/cleavage target pairs using degradome libraries prepared from four tissues and three temperatures with CleaveLand4 (Brousse et al., 2014; p-value cutoff >= 0.1, category cutoff <= 3), including 145 category 0 hits (Table 2).

Temperature regulated miRNAs were identified by filtering for sequences that had abundances more than 40 RPM in any libraries and changed more than 1.5-fold between temperatures. This filtering step resulted in 50 temperature regulated miRNA sequences (Figure 10), including isomiRs of known sequences. Many of the temperature regulated miRNA sequences show clear tissue-specific expression pattern. A good example is mir780, which mainly is expressed in flowers (Figure 10).

We used northern blot assay to confirm the results of our bioinformatic analysis about the temperature regulated expression of Arabidopsis miRNAs in the different tissues (seedling, root, leaf, and flower). Those miRNAs that gave signal on the northern blot, in most cases were detectable in all of the tissues tested and they were temperature regulated (Figure 11).

Interestingly, many of the de novo predicted mature miRNA sequences are not the same as the miRBase mature sequence. Sometimes the “star” sequence is more abundant than the “mature”. This phenomenon has been described by others as well, leading to the conclusion that the nomenclature using “mature” and “star” for the most abundant and the corresponding antiparallel sequence is outdated, because the Argonaute enzyme can cleave either one of them depending on yet unknown regulatory processes. One example is the mir169f-3p, which is considered the “star” sequence, however, it is roughly 10 times more abundant in our libraries than the canonical mir169f-5p “mature” sequence and is strongly temperature dependent, decreasing in higher temperature. Interestingly, we have identified a 0 category target (AT1G49910, BUB3.2, BUDDING UNINHIBITED BY BENZYMIDAZOL) for this sequence by using our degradome libraries. This WD40-domain containing protein is part of a Cul4 RING E3 ubiquitin ligase complex and can be found in mitotically active cells (Lermontova et al., 2008).We also found few temperature-regulated non-conserved miRNAs. For example the Arabidopsis specific miRNA779 was downregulated at higher temperature in every tissue (Figure 10).

We identified the mRNAs that were cleaved by the temperature regulated miRNAs in our degradome libraries. Next we also performed the GO enrichment analysis of the temperature

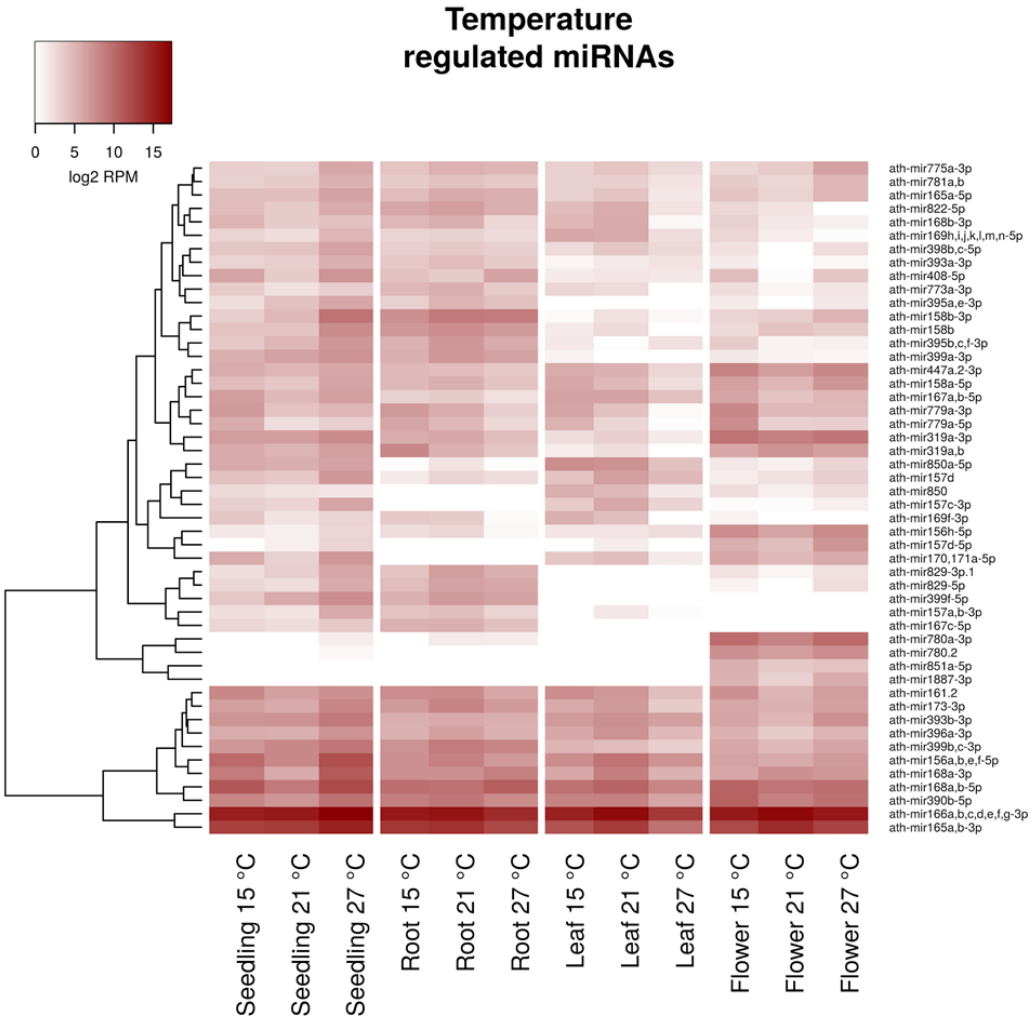

Figure 10. Heatmap of temperature regulated miRNAs in different tissues.
Nonredundant miRNA sequences from miRBase v21 and the mature and star sequences of ShortStack predicted miRNA loci were merged and their differential expression upon temperature change was measured. Only sequences with more than 40 RPM maximum value in any samples that changed at least 1.5× between temperatures were kept and listed.

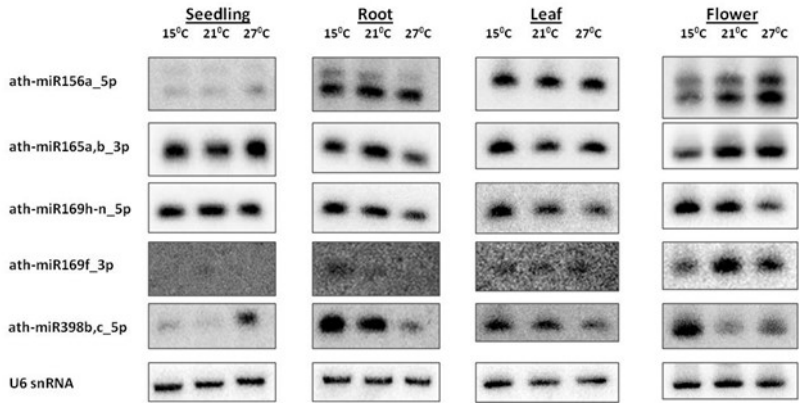

Figure 11. Northern blot analysis of selected temperature regulted miRNAs in different tissues. Total RNA was extracted from different tissues including, seedling, root, leaf and flower from Arabidopsis plants. The RNA was separated on PAGE and transferred to nylon membranes for Northern blot analysis of the temperature regulated miRNAs. Oligonucleotide probes were used to detect specific miRNAs, and an U6-specific probe was used to detect U6 RNA as a loading control for each membrane.

Query	Transcript	Slice position	MFE ratio	Allen score	Category	p-value
ath-mir156a,b,e,f-5p	AT1G27360.1 SPL11 squamosa promoter-like 11	1263	0,938	1	0	0,001
ath-mir156a,b,e,f-5p	AT1G69170.1 Squamosa promoter-binding protein-like SBP domain transcription factor family protein	1307	0,938	1	0	0,002
ath-mir156a,b,e,f-5p	AT2G33810.1 SPL3 squamosa promoter binding protein-like 3	797	0,909	1,5	0	0,009
ath-mir156a,b,e,f-5p	AT3G15270.1 SPL5 squamosa promoter binding protein-like 5	655	0,828	3	0	0,011
ath-mir156a,b,e,f-5p	AT3G21300.1 RNA methyltransferase family protein	1249	0,685	5,5	0	0,059
ath-mir156a,b,e,f-5p	AT5G50570.2 SPL13A SPL13 Squamosa promoter-binding protein-like SBP domain transcription factor family protein	977	0,925	1	0	0,008
ath-mir156h-5p	AT1G07960.1 ATPDIL5.1 PDIL5.1 PDI-like 5.1	23	0,658	8	0	0,082
ath-mir156h-5p	AT2G42200.1 SPL9 AtSPL9 squamosa promoter binding protein-like 9	948	0,938	2	0	0,005
ath-mir156h-5p	AT3G57920.1 SPL15 squamosa promoter binding protein-like 15	856	0,938	2	0	0,004
ath-mir156h-5p	AT5G43270.1 SPL2 squamosa promoter binding protein-like 2	1199	0,944	2	2	0,066
ath-mir157d	AT1G27360.2 SPL11 squamosa promoter-like 11	1223	0,932	2	0	0,002
ath-mir157d	AT1G27370.4 SPL10 squamosa promoter binding protein-like 10	1325	0,929	2	0	0,003
ath-mir157d	AT1G53160.1 SPL4 squamosa promoter binding protein-like 4	602	0,839	3	0	0,009
ath-mir157d	AT5G50670.1 SPL13B SPL13 Squamosa promoter-binding protein-like SBP domain transcription factor family protein	1112	0,918	2	0	0,008
ath-mir157d	AT1G27360.3 SPL11 squamosa promoter-like 11	1250	0,932	2	2	0,066
ath-mir157d-5p	AT1G27360.4 SPL11 squamosa promoter-like 11	1311	0,873	3	0	0,002
ath-mir157d-5p	AT1G27370.2 SPL10 squamosa promoter binding protein-like 10	1457	0,871	3	0	0,006
ath-mir157d-5p	AT1G69170.1 Squamosa promoter-binding protein-like SBP domain transcription factor family protein	1308	0,929	2	2	0,066
ath-mir158b	AT1G62860.1 pseudogene of pentatricopeptide PPR repeat-containing protein	425	0,848	3	2	0,066
ath-mir161.2	AT1G62910.1 Pentatricopeptide repeat PPR superfamily protein	997	0,912	3	0	0,002
ath-mir161.2	AT4G04780.1 MED21 mediator 21	132	0,662	7,5	0	0,056
ath-mir161.2	AT5G41170.1 Pentatricopeptide repeat PPR-like superfamily protein	892	0,861	3	0	0,005
ath-mir165a,b-3p	AT1G30490.1 PHV ATHB9 Homeobox-leucine zipper family protein lipid-binding START domain-containing protein	806	0,867	3	0	0,001
ath-mir165a,b-3p	AT2G34710.1 PHB ATHB14 ATHB.14 PHB.1D Homeobox-leucine zipper family protein lipid-binding START domain-containing protein	881	0,867	3	0	0,001
ath-mir165a,b-3p	AT4G32880.1 ATHB-8 ATHB8 HB-8 homeobox gene 8	945	0,867	3	0	0,002
ath-mir165a,b-3p	AT5G60690.1 REV IFL IFL1 Homeobox-leucine zipper family protein lipid-binding START domain-containing protein	1273	0,867	3	0	0,002
ath-mir166a,b,c,d,e,f,g-3p	AT1G52150.1 ATHB.15 ATHB15 CNA ICU4 Homeobox-leucine zipper family protein lipid-binding START domain-containing protein	1279	0,859	3	0	0,001
ath-mir166a,b,c,d,e,f,g-3p	AT1G52150.2 ATHB.15 ATHB15 CNA ICU4 Homeobox-leucine zipper family protein lipid-binding START domain-containing protein	1279	0,859	3	0	0,001
ath-mir167c-5p	AT4G27090.1 Ribosomal protein L14	400	0,673	28	0	0,080
ath-mir167c-5p	AT1G49290.1 unknown protein	710	0,683	9	1	0,010
ath-mir168a,b-5p	AT1G48410.3 AGO1 Stabilizer of iron transporter SufD Polynucleotidyl transferase	532	0,792	5	0	0,001
ath-mir168a,b-5p	AT1G48410.2 AGO1 Stabilizer of iron transporter SufD Polynucleotidyl transferase	522	0,792	5	2	0,066
ath-mir169f-3p	AT1G49910.1 BUB3.2 Transducin WD40 repeat-like superfamily protein	1051	0,688	6	0	0,033
ath-mir169h,i,j,k,l,m,n-5p	AT1G17590.2 NF-YA8 nuclear factor Y subunit A8	1210	0,868	2,5	0	0,002
ath-mir169h,i,j,k,l,m,n-5p	AT1G17590.3 NF-YA8 nuclear factor Y subunit A8	1621	0,868	2,5	0	0,002
ath-mir169h,i,j,k,l,m,n-5p	AT1G48500.2 JAZ4 TIFY6A jasmonate-zim-domain protein 4	975	0,661	4	0	0,072
ath-mir169h,i,j,k,l,m,n-5p	AT1G54160.1 NFYA5 NF-YA5 nuclear factor Y subunit A5	1295	0,853	1,5	0	0,004
ath-mir169h,i,j,k,l,m,n-5p	AT1G72830.3 HAP2C ATHAP2C NF-YA3 nuclear factor Y subunit A3	1424	0,860	2,5	0	0,003
ath-mir169h,i,j,k,l,m,n-5p	AT3G05690.1 UNE8 ATHAP2B HAP2B NF-YA2 nuclear factor Y subunit A2	1194	0,786	3	0	0,005
ath-mir169h,i,j,k,l,m,n-5p	AT5G06510.1 NF-YA10 nuclear factor Y subunit A10	1078	0,786	3	0	0,005
ath-mir169h,i,j,k,l,m,n-5p	AT5G12840.4 HAP2A ATHAP2A NF-YA1 nuclear factor Y subunit A1	1130	0,683	5	0	0,043
ath-mir169h,i,j,k,l,m,n-5p	AT1G17590.4 NF-YA8 nuclear factor Y subunit A8	1516	0,868	2,5	2	0,066
ath-mir170,171a-5p	AT2G01990.1 unknown protein	623	0,729	11	0	0,007
ath-mir319a,b	AT1G53230.1 TCP3 TEOSINTE BRANCHED 1 cycloidea and PCF transcription factor 3	1195	0,748	4	0	0,011
ath-mir319a,b	AT3G15030.1 TCP4 MEE35 TCP family transcription factor 4	1487	0,757	3,5	0	0,008
ath-mir319a,b	AT3G66658.2 ALDH22A1 aldehyde dehydrogenase 22A1	1112	0,711	3,5	0	0,018
ath-mir319a,b	AT5G18065.1 unknown protein	656	0,678	15	0	0,031
ath-mir390b-5p	AT1G56130.1 Leucine-rich repeat transmembrane protein kinase	348	0,684	5	0	0,031
ath-mir390b-5p	AT5G57735.1 TASIR-ARF tasiR-ARF	429	0,675	4,5	0	0,041
ath-mir393a-3p	AT4G32520.2 SHM3 serine hydroxymethyltransferase 3	1037	0,845	4,5	2	0,066
ath-mir393b-3p	AT1G69040.1 ACR4 ACT domain repeat 4	573	0,690	12	0	0,098
ath-mir395a,e-3p	AT1G50930.1 unknown protein	53	0,821	2	0	0,003
ath-mir395a,e-3p	AT3G22890.1 APS1 ATP sulfurylase 1	453	0,798	3,5	0	0,004
ath-mir395a,e-3p	AT5G43780.1 APS4 Pseudouridine synthase archaeosine transglycosylase-like family protein	406	0,903	1,5	2	0,066
ath-mir399a-3p	AT2G33770.1 UBC24 ATUBC24 PHO2 phosphate 2	840	0,939	2	2	0,066
ath-mir399b,c-3p	AT2G33770.1 UBC24 ATUBC24 PHO2 phosphate 2	751	0,864	2,5	2	0,066
ath-mir399f-5p	AT4G34138.1 UGT73B1 UDP-glucosyl transferase 73B1	1294	0,776	9	2	0,066
ath-mir773a-3p	AT4G28200.1 FUNCTIONS IN molecular function unknown	1896	0,682	7	1	0,048
ath-mir773a-3p	AT4G14140.1 MET2 DMT02 DMT2 MET02 DNA methyltransferase 2	21	0,940	2	2	0,066

Table 3. Experimentally validated targets of the temperature regulated Arabidopsis miRNAs

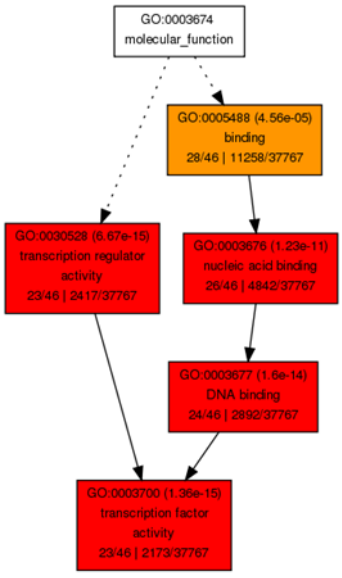

Figure 12. GO enrichment analysis of the temperature regulated miRNA's target genes.

regulated miRNA's target genes. Among the experimentally identified targets we found significant enrichment for the GO terms of nucleic acid binding, DNA binding, transcription regulator activity and transcription factor activity. These findings may suggest that the temperature regulated miRNAs serves as master regulators in temperature dependent gene expression regulation.

3.2. MiR169 is ambient temperature regulated

One of the temperature regulated miRNAs is the miR169 family that we investigated in more details. The miR169 family is evolutionary conserved and it has been identified in more than 40 species (Sunkar and Jagadeeswaran, 2008). The miR169 family often makes up the largest miRNA family. In Arabidopsis four isoforms of miR169 are encoded by 14 different genes (Figure 13). The miR169 isoforms show distinct expression patterns during development (Gonzales et al., 2011; Sorin et al., 2014), in response to abiotic (Licausi et al., 2011; Zhao et al., 2011) or biotic stresses (Singh et al., 2012), suggesting a functional specialization.

Members	Mature sequences	Chromosome
Mir169a	CAGCCAAGGATGACTTGCCGA	3
Mir169b/c	CAGCCAAGGATGACTTGCCGG	5
Mir169d/e/f/g	TGAGCCAAGGATGACTTGCCG	1,3,1,4
Mir169h/i/j/k/l/m/n	TAGCCAAGGATGACTTGCCTG	1,3,3,3,3,3,3

Figure 13. The mature sequences of the Arabidopsis miR169 family with the chromosomal location. The identical nucleotides of the miR169 isoforms are marked in red.

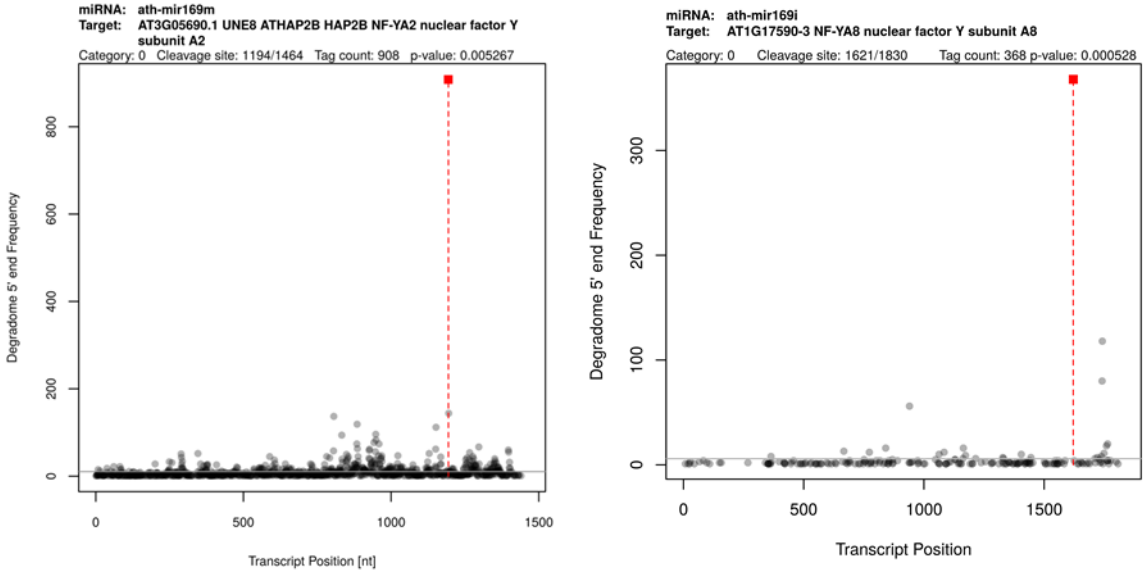

Figure 14. Target plots (t-plots) of miR169 targets confirmed by degradome sequencing. In the head of the pictures there is a unique identifier of the mRNA followed by the annotation of the transcript. The relative degradome tag abundances are plotted against the nucleotide position within the transcript.

The miR169 family target diverse mRNAs, encoding subunits A of the Nuclear Factor Y (NF-Y) transcription factor complex. We also identified NF-Y mRNAs that were cleaved by miR169 in our degradome libraries (Figure 14). This transcription factor (TF) is a conserved heterotrimeric TF complex and it is composed of NF-YA, NF-YB and NF-YC subunits (Petroni et al., 2012). The NF-YB and NF-YC subunit contain a histone fold domain, which is very similar to H2A and H2B core histones. NF-Ys are sequence-specific transcription factors and recognize the CCAAT motif in eukaryotic promoters. The Arabidopsis genome contains 10 NF-YA, 10 NF-YB and 10 NF-YC subunits and they could theoretically combine to form 1000 unique complexes (Figure 15).

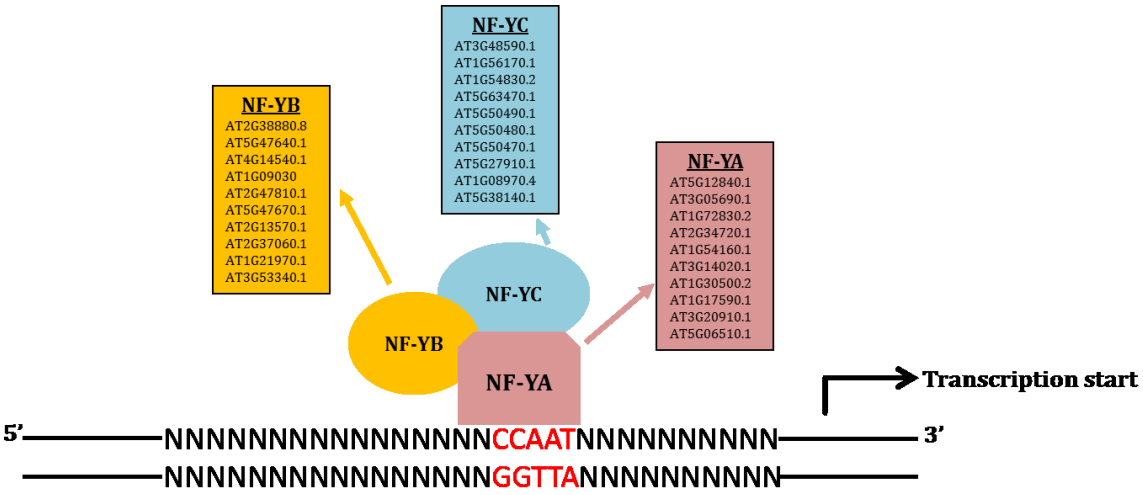

Figure 15. Nuclear Factor Y transcription factors in Arabidopsis.

Plant development is responsive to temperature and plants can measure temperature very accurately and can distinguish as little differences as 1 ^{o}C. Warm temperature promote early flowering and it was shown that in Arabidopsis the NF-Y complex (composed of NF-YA2, NF-YB2 and NF-YC9) control flowering time by integrating environmental and developmental signals. It was shown that a NF-Y complex (composed of NF-YA2, NF-YB2 and NF-YC9) interacts with Constans (CO) in the photoperiod pathway and DELLAs in the gibberellin pathway, to directly regulate the transcription of SOC1, a major floral pathway integrator (Hou et al., 2014). The SOC1 floral integrator is a member of the MADS box TF family and trigger the floral transition at the right moment during plant development and under environmental conditions that are favourable for reproduction (Figure 16).

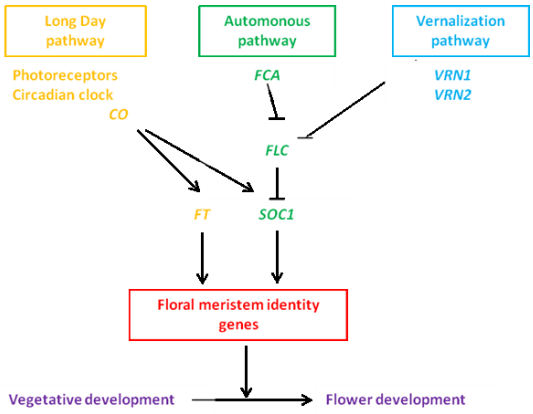

Figure 16. Simple model of flowering time regulation in Arabidopsis.

We found that Arabidopsis plants grown at 15 °C flowers significantly later than at higher ambient temperatures (Figure 1) and in their rosette leaves the expression level of the SOC1 floral pathway integrator was lower than at higher ambient temperatures (Figure 18). The expression level of SOC1 is regulated by the NF-Y TF complex. Furthermore the NF-YA2 component of the SOC1 regulating NF-Y TF complex is regulated by miR169h-n. In line with flowering time and SOC1 expression level we also found that the negative regulator of NF-YA2 (miR169h-n isoforms) shows temperature regulated expression pattern and has high expression level at 15 °C and expresses lowly at 27 °C (Figure 17).

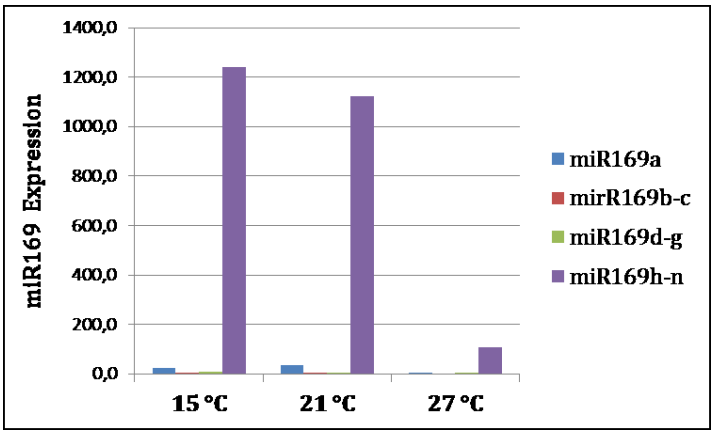

Figure 17. The miR169h-n isoform is ambient temperature regulated

A

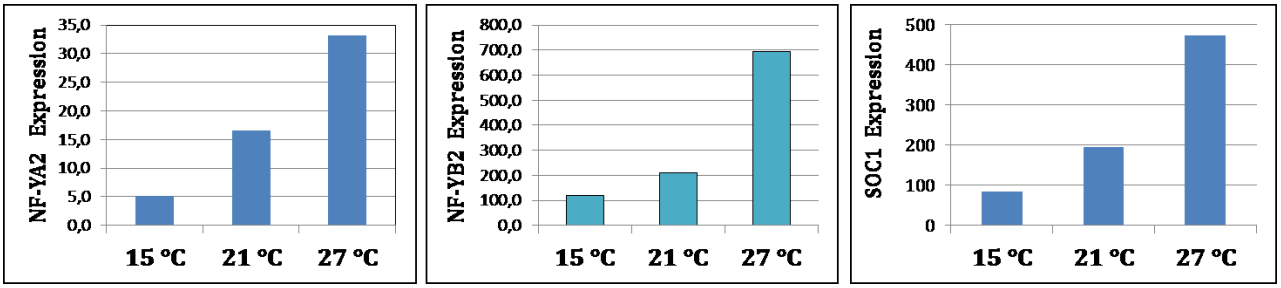

B

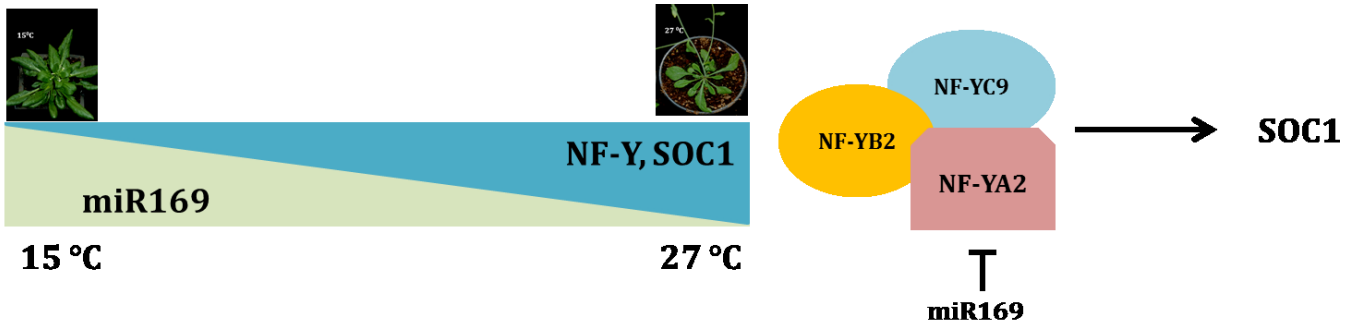

Figure 18. A proposed model for flowering time regulation by miR169h-n. (A) NF-YA2 is down-regulated by miR169h-n at low ambient temperature. (B) miR169h-n level decreases with temperature increasing therefore it promotes flowering via SOC1 regulation at higher ambient temperatures.

Furthermore we experimentally identified and validated that indeed the miR169h-n cleaved the NF-YA2 mRNAs (Figure 14). The NF-YB2 component of the NF-Y TF complex also shows a temperature regulated expression pattern, however it is independent of miR169 regulation.

Based on these observations we propose miR169h-n could mediate ambient temperature signals during inductive photoperiod to modify flowering time via SOC1.

3.3. Identification of temperature regulated 21 nt and 24 nt long pha-siRNAs

In plants a few usually 22 nt long miRNA can trigger the production of pha-siRNAs from target transcripts (Fei et al., 2013). Target RNA produced from PHAS loci is cleaved by miRNA-guided AGO and either the 5' or 3' cleavage fragment is converted by RDR6 to double stranded RNA, which is then successively diced into 21-nt pha-siRNAs. The phasing register of the loci is determined by miRNA-guided cleavage. Originally in Arabidopsis, eight noncoding TAS loci were described. Since these TAS loci derived phasiRNAs regulate target genes in *trans*, they are also termed as trans-acting siRNAs (ta-siRNAs). In addition to the noncoding TAS loci, protein-coding genes such as NBS-LRR and pentatricopeptide repeat (PPR) genes are also targeted by 22-nt long miRNAs and produce phasiRNAs (Howell et al., 2007).

In our sRNA libraries we identified pha-siRNA loci that were temperature regulated. First we identified the "classical" pha-siRNA producing loci that produced 21 nt long pha-siRNAs (Figure 19). Among the top 50 temperature regulated 21 nt pha-siRNA cluster we found the members of TAS loci (TAS1, TAS2, TAS3, TAS4). These TAS loci were also the most abundant pha-siRNA producing loci. Many pha-siRNA producing loci showed also tissue specific expression pattern. Most of the pha-siRNA producing loci were down regulated with the temperature increasing, however there were loci which produced more pha-siRNAs at higher ambient temperature (eg. Cluster 66929) (Figure 19).

We also identified pha-siRNA producing loci that produced 24 nt long pha-siRNAs (Figure 20). The vast majority of the top 50 temperature regulated 24 nt pha-siRNA cluster were located on transposable elements. These 24 nt long pha-siRNA producing loci showed also tissue specific expression pattern and they were most abundant in flowers. Most of the 24 nt long pha-siRNA producing loci were down regulated in leaf and root with the temperature increasing and they showed opposite expression pattern in seedlings (Figure 20).

We identified the mRNAs that were cleaved by the temperature regulated pha-siRNAs in our degradome libraries. Next we also performed the GO enrichment analysis of the temperature regulated pha-siRNA's target genes. Among the experimentally identified targets we found significant enrichment for the GO terms of post-embryonic development (Figure 21). These findings may suggest that the temperature regulated pha-siRNAs could help to adapt the plants post embryonic development to changing temperature.

A

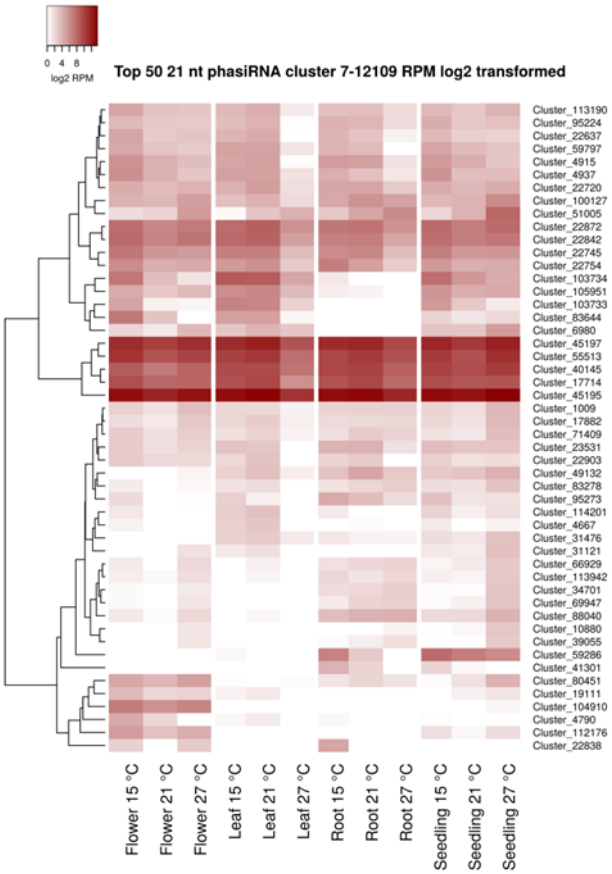

B

Name	Locus	Annotation_gene_name
Cluster_45195	chr2:16536816-16538283	TAS1C
Cluster_45197	chr2:16539045-16540443	TAS2
Cluster_55513	chr3:5861462-5862674	TAS3/TASIR-ARF (TRANS-ACTING SIRNA3)
Cluster_40145	chr2:11720653-11722519	TAS1A
Cluster_22872	chr1:23413088-23415154	Transacting siRNA generating locus. Itself is targeted by TAS2-derived ta-siR2140 for cleavage.
Cluster_22842	chr1:23388221-23390366	Transacting siRNA generating locus. Is targeted by TAS2-derived ta-siR2140 for cleavage.
Cluster_59286	chr3:9417447-9417825	TAS4
Cluster_4937	chr1:4368374-4370243	auxin signaling F-box 3
Cluster_112176	chr5:23394138-23394560	tasiR-ARF
Cluster_113190	chr5:24308533-24309764	auxin response factor 4
Cluster_31476	chr2:855026-856667	phytochrome kinase substrate 1

Figure 19. Heatmap (A) and annotaions (B) some of the temperature regulated 21 nt long pha-siRNAs in different tissues.

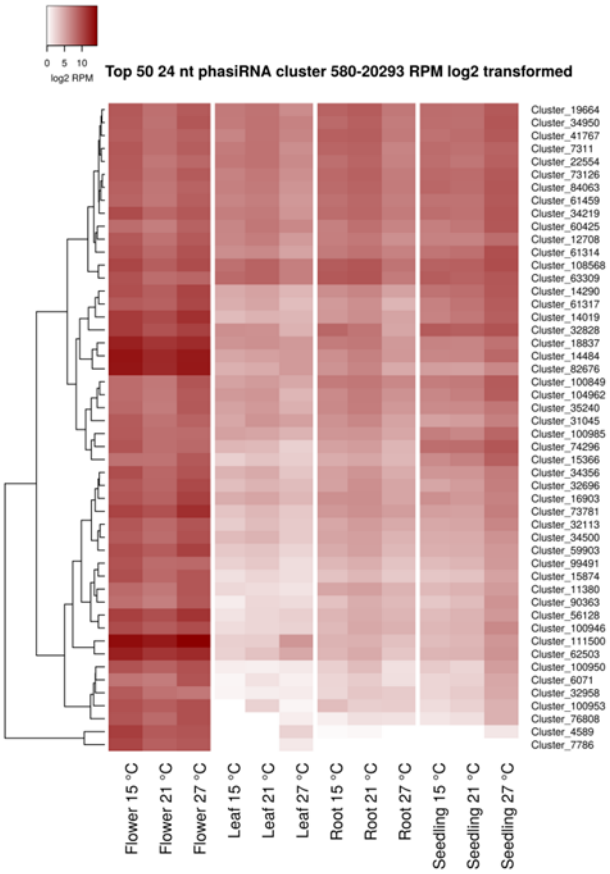

Name	Locus	Annotation_gene_type
Cluster_14484	chr1:13565906-13577184	transposable_element
Cluster_82676	chr4:12840861-12845520	transposable_element
Cluster_18837	chr1:19575857-19578571	transposable_element
Cluster_62503	chr3:14314407-14317572	transposable_element
Cluster_73781	chr4:2525843-2527507	transposable_element
Cluster_14019	chr1:12898346-12903613	transposable_element
Cluster_56128	chr3:6431520-6433198	transposable_element
Cluster_32828	chr2:2520452-2533379	transposable_element
Cluster_59903	chr3:9965084-9966903	transposable_element
Cluster_16903	chr1:17823259-17825465	transposable_element
Cluster_14290	chr1:13236890-13245441	transposable_element
Cluster_7786	chr1:6947451-6948602	transposable_element
Cluster_61317	chr3:11437006-11438573	transposable_element
Cluster_32696	chr2:2262210-2266066	transposable_element
Cluster_34219	chr2:5981407-6002295	transposable_element
Cluster_34356	chr2:6216518-6224968	transposable_element
Cluster_15874	chr1:16801399-16803473	transposable_element
Cluster_61314	chr3:11402675-11425396	transposable_element
Cluster_76808	chr4:7250434-7251274	transposable_element
Cluster_34500	chr2:6397391-6398997	transposable_element
Cluster_99491	chr5:9178450-9178899	transposable_element
Cluster_32113	chr2:1482360-1484979	transposable_element
Cluster_74296	chr4:3518221-3531634	transposable_element
Cluster_100849	chr5:10905467-10924920	transposable_element
Cluster_11380	chr1:10382910-10384502	transposable_element
Cluster_19664	chr1:20311747-20321039	transposable_element
Cluster_41767	chr2:13374401-13375741	transposable_element
Cluster_35240	chr2:7277912-7279140	transposable_element
Cluster_73126	chr4:1486202-1487756	transposable_element
Cluster_15366	chr1:15960678-15965040	transposable_element
Cluster_61459	chr3:11703027-11715527	transposable_element
Cluster_100985	chr5:11324000-11328663	transposable_element
Cluster_22554	chr1:23117959-23123594	transposable_element
Cluster_32958	chr2:2889677-2891914	transposable_element

Figure 20. Heatmap and annotaions of the temperature regulated 24 nt long pha-siRNAs in different tissues.

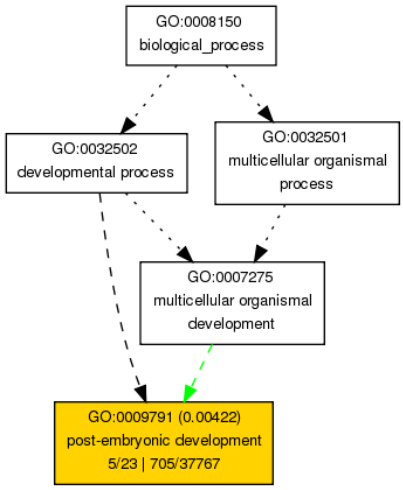

Figure 21. GO enrichment analysis of the temperature regulated pha-siRNA's target genes.

3.4. 24-nt-long heterochromatic siRNAs

Most of the *de novo* predicted sRNA clusters have a dominant sequence size of 24-nt (41240, 35.5%). The mechanism of production of 24-nt-long siRNAs can be diverse. One class of

siRNAs is produced from PolIV-dependent short transcripts. These transcripts are immediately subjected to RDR2-dependent complementary RNA synthesis and DCL3-mediated cleavage. These cleaved, perfectly complementary double stranded siRNAs are then loaded into RITS complexes keeping one strand while eliminating the other. This active complex is then recruited to PolV-dependent transcripts (PolV has an AGO-interacting domain) where they promote the assembly of DNA methylating protein complexes and initiate *de novo* methylation of DNA at closely localised asymmetric CHG and CHH sites. The 24-nt-long class of siRNAs usually derive from repetitive and/or transposable elements and their function is to repress their expression through guiding DNA methylation at these sites and therefore prevent genomic instability. This is extremely important in reproductive tissues and germlines which is reflected in the increase of ratio of this size class compared to the 21-nt-long class in flowers (Figure 21, panel D).

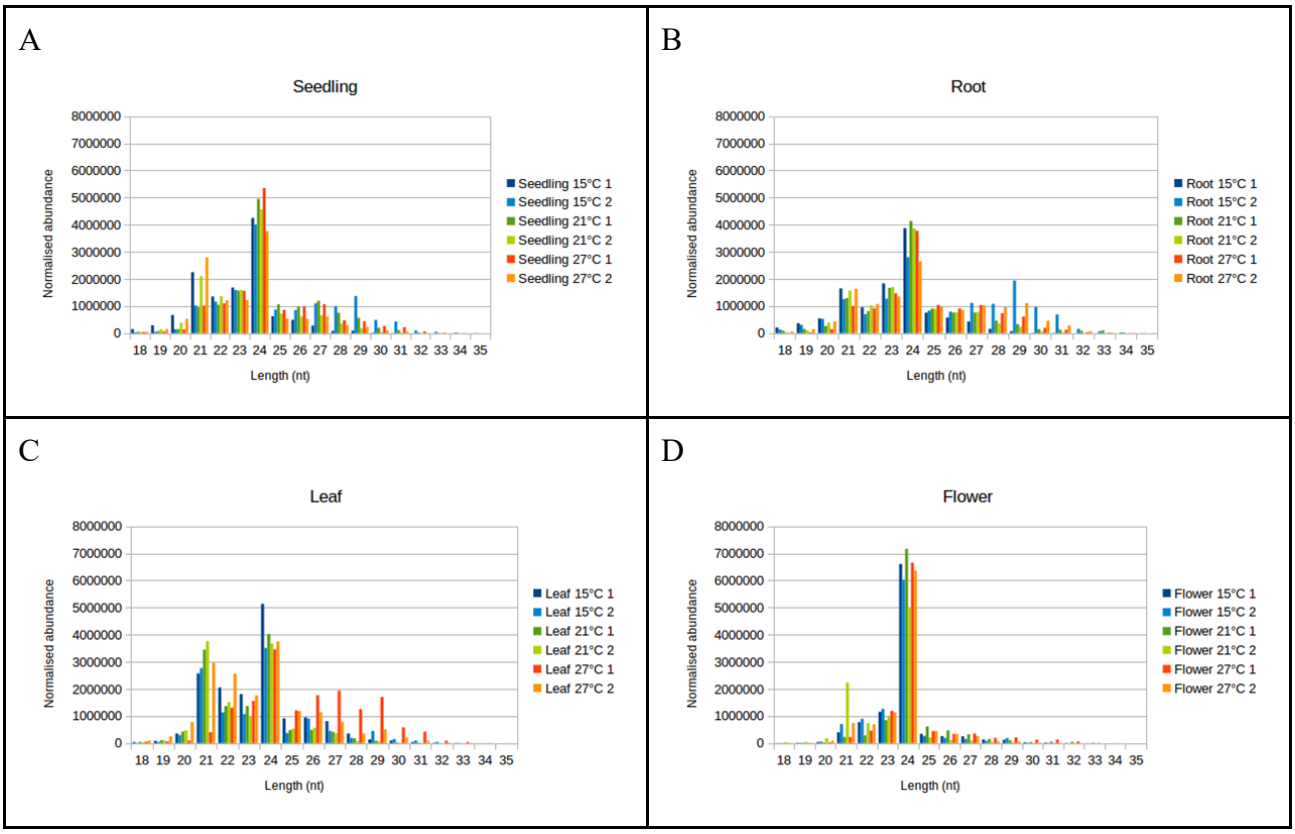

Figure 21. Size distribution of sRNAs in various tissues at different ambient temperatures.
Small RNA sequences were mapped to the Arabidopsis thaliana TAIR10 genome using ShortStack. Genome matching sequences of size classes from 18-nt to 35-nt were counted, normalised and the values were plotted in all four tissues sampled at three ambient temperatures.

At global scale, there is no significant change can be seen in the level of 24-nt-long siRNAs. The same conclusion can be drawn when the genomic location of the 24-nt-long sequences are visualised (Figure 22). However, there are clearly temperature dependent 24-nt-long clusters at distinct sites which are usually associated with transposons.

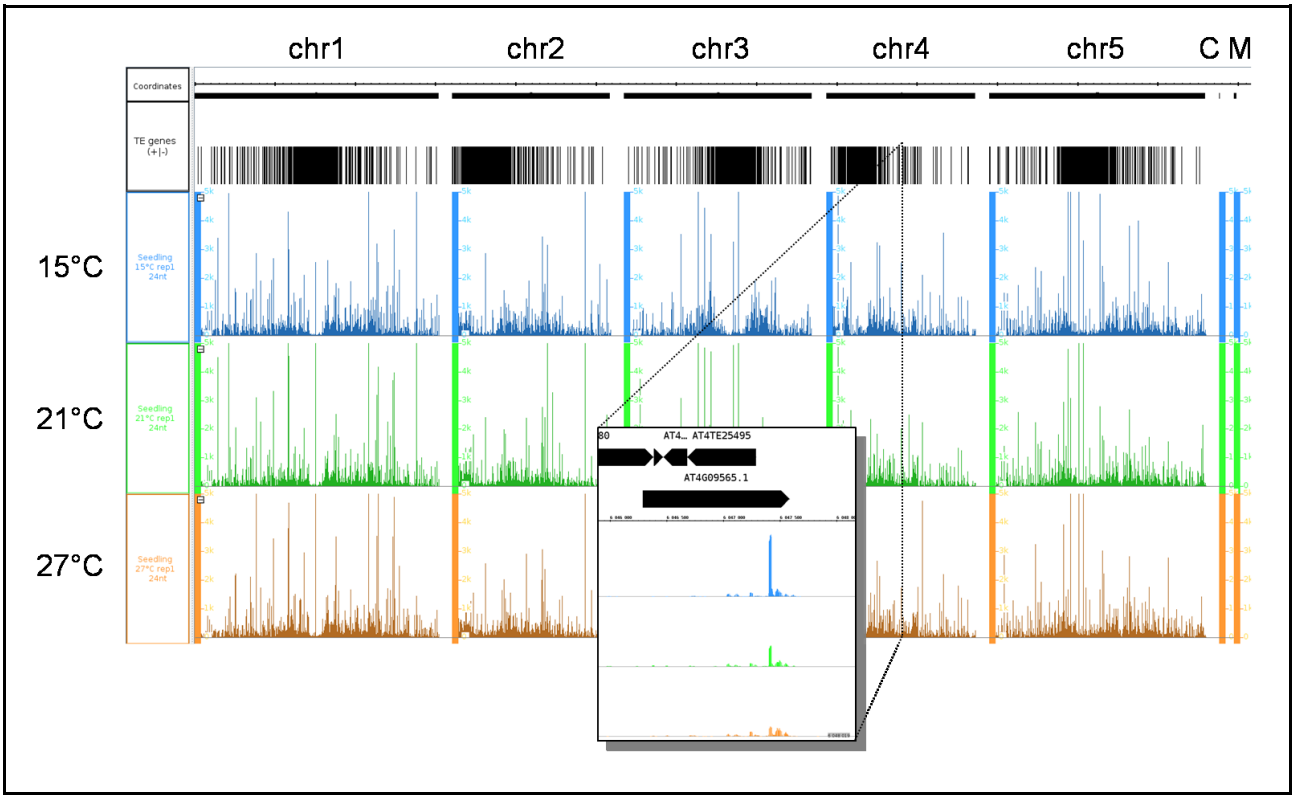

Figure 22. Genome-wide distribution of 24-nt siRNAs.
Small RNA sequences were mapped to the Arabidopsis thaliana TAIR10 genome using ShortStack. 24-nt-long sequences were filtered from the alignment file and converted to bedgraph format using samtools and bedtools. The abundances were normalised and the tracks were visualised with Integrated Genome Browser along with the distribution of transposon genes.

The siRNA distribution was measured at every known transposon genes according to the TAIR10 genome annotation. Again, in most of the tissues the global siRNA distribution did not change significantly, except for the leaf tissue, where the total siRNA production dropped at higher ambient temperatures (Figure 23, panel A). The number of transposon genes with significantly different siRNA production could be observed at higher temperature, especially in the flower and the seedling. In flowers, most of the transposons that were associated with significantly changed siRNA production belonged to the LTR/Gypsy superfamily, whereas in the seedling, almost every superfamily was represented.

4. References

Addo-Quaye, C., Miller, W., Axtell, M.J. (2009). CleaveLand: a pipeline for using degradome data to find cleaved small RNA targets. Bioinformatics 25, 130-131.

Andrews S. (2010). FastQC: a quality control tool for high throughput sequence data. Available online at:http://www.bioinformatics.babraham.ac.uk/projects/fastqc

Argyris, J., Truco, M.J., Ochoa, O., Knapp, S.J., Still, D.W., Lenssen, G.M., Schut, J.W., Michelmore, R.W., and Bradford, K.J. (2005). Quantitative trait loci associated with seed and seedling traits in Lactuca. Theor Appl Genet *111*, 1365-1376.

Aukerman, M.J., and Sakai, H. (2003). Regulation of flowering time and floral organ identity by a MicroRNA and its APETALA2-like target genes. Plant Cell 15, 2730-2741.

Axtell, M.J. (2014). Butter: High-precision genomic alignment of small RNA-seq data. bioRxiv 7427.

Baksa, I., Nagy, T., Barta, E., Havelda, Z., Várallyay, É., Silhavy, D., Burgyán, J. and Szittya, G. (2015). Identification of Nicotiana benthamiana microRNAs and their targets using high throughput sequencing and degradome analysis. BMC Genomics, 16:1025. doi: 10.1186/s12864-015-2209-6.

Brodersen, P., Sakvarelidze-Achard, L., Bruun-Rasmussen, M., Dunoyer, P., Yamamoto, Y.Y., Sieburth, L., and Voinnet, O. (2008). Widespread translational inhibition by plant miRNAs and siRNAs. Science 320, 1185-1190.

Brousse, C., Liu, Q., Beauclair, L., Deremetz, A., Axtell, M.J., and Bouché, N. (2014). A non-canonical plant microRNA target site. Nucl Acids Res 42, 5270–5279.

Carthew, R.W., and Sontheimer, E.J. (2009). Origins and Mechanisms of miRNAs and siRNAs. Cell 136, 642-655.

Chen, X. (2004). A microRNA as a translational repressor of APETALA2 in Arabidopsis flower development. Science 303, 2022-2025.

Ding, S.W., and Voinnet, O. (2007). Antiviral immunity directed by small RNAs. Cell 130, 413-426.

Du, Z., Zhou, X., Ling, Y., Zhang, Z., and Su, Z. (2010). agriGO: a GO analysis toolkit for the agricultural community. Nucleic Acids Res 38, W64–W70.

Fei, Q., R. Xia, and B.C. Meyers, Phased, secondary, small interfering RNAs in posttranscriptional regulatory networks. (2013). Plant Cell, 25, 2400-2415.

Gasciolli, V., Mallory, A.C., Bartel, D.P., and Vaucheret, H. (2005). Partially redundant functions of Arabidopsis DICER-like enzymes and a role for DCL4 in producing trans-acting siRNAs. Curr. Biol. 15, 1494-1500.

German, M.A., Luo, S., Schroth, G., Meyers, B.C., and Green, P.J. (2009). Construction of Parallel Analysis of RNA Ends (PARE) libraries for the study of cleaved miRNA targets and the RNA degradome. Nat. Protocols 4, 356–362.

Gonzalez-Ibeas D, Blanca J, Donaire L, Saladie M, Mascarell-Creus A, Cano-Delgado A, Garcia-Mas J, Llave C, Aranda M. (2011). Analysis of the melon (Cucumis melo) small RNAome by high-throughput pyrosequencing. BMC genomics 12: 393.

Hou, X., Zhou, J., Liu, C., Liu, J., Shen, L., Yu, H. (2014). Nuclear factor Y-mediated H3K27me3 demethylation of the SOC1 locus orchestrates flowering responses of Arabidopsis. Nature Communications 5, 4601.

Howell, M.D., Fahlgren, N., Chapman, E.J., Cumbie, J.S., Sullivan, C.M., Givan, S.A., Kasschau, K.D., and Carrington, J.C. (2007). Genome-wide analysis of the RNA-DEPENDENT RNA POLYMERASE6/DICER-LIKE4 pathway in Arabidopsis reveals dependency on miRNA- and tasiRNA-directed targeting. Plant Cell 19, 926-42

Johnson, N.R., Yeoh, J.M., Coruh, C., and Axtell, M.J. (2016). Improved Placement of Multi-Mapping Small RNAs. bioRxiv 44099.

Kasschau, K.D., Fahlgren, N., Chapman, E.J., Sullivan, C.M., Cumbie, J.S., Givan, S.A., and Carrington, J.C. (2007). Genome-wide profiling and analysis of Arabidopsis siRNAs. PLoS Biol. 5, 0479-0493.

Keam, S. P. and Hutvagner, G. (2015). tRNA-Derived Fragments (tRFs): Emerging New Roles for an Ancient RNA in the Regulation of Gene Expression. Life 5, 1638–1651; doi:10.3390/life5041638

Kumar, S.V., and Wigge, P.A. (2010). H2A.Z-containing nucleosomes mediate the thermosensory response in Arabidopsis. Cell 140, 136-147.

Lam, F.H., Steger, D.J., and O'Shea, E.K. (2008). Chromatin decouples promoter threshold from dynamic range. Nature 453, 246-250.

Lee, H., Yoo, S.J., Lee, J.H., Kim, W., Yoo, S.K., Fitzgerald, H., Carrington, J.C., and Ahn, J.H. (2010). Genetic framework for flowering-time regulation by ambient temperature-responsive miRNAs in Arabidopsis. Nucleic Acids Res. 38, 3081-3093.

Lermontova, I., Fuchs, J., and Schubert, I. (2008). The Arabidopsis checkpoint protein Bub3.1 is essential for gametophyte development. Front. Biosci. 13, 5202–5211.

Licausi F, Weits DA, Pant BD, Scheible WR, Geigenberger P, Van Dongen JT. (2011). Hypoxia responsive gene expression is mediated by various subsets of transcription factors and miRNAs that are determined by the actual oxygen availability. New phytologist 190: 442–456.

Llave, C., Xie, Z., Kasschau, K.D., and Carrington, J.C. (2002). Cleavage of Scarecrow-like mRNA targets directed by a class of Arabidopsis miRNA. Science 297, 2053-2056.

Martin, M. (2011). Cutadapt removes adapter sequences from high-throughput sequencing reads. EMBnet.journal 17, 10–12.

McCormick, K.P., Willmann, M.R., and Meyers, B.C. (2011). Experimental design, preprocessing, normalization and differential expression analysis of small RNA sequencing experiments. Silence 2, 2.

Mosher, R.A., Schwach, F., Studholme, D., and Baulcombe, D.C. (2008). PolIVb influences RNA-directed DNA methylation independently of its role in siRNA biogenesis. Proc. Natl. Acad. Sci. USA 105, 3145-3150.

Penfield, S. (2008). Temperature perception and signal transduction in plants. New Phytol. 179, 615-628.

Peragine, A., Yoshikawa, M., Wu, G., Albrecht, H.L., and Poethig, R.S. (2004). SGS3 and SGS2/SDE1/RDR6 are required for juvenile development and the production of trans-acting siRNAs in Arabidopsis. Genes Dev. 18, 2368-2379.

Petroni, K., Kumimoto, R.W., Gnessuta, N., Calvenzani, V., Fornari, M., Tonelli, C., Holt, B.F., Mantovani, R. (2012) The promiscuous life of plant Nuclear Factor Y transcription factors. The Plant Cell, 24, 4777-4792.

Quinlan, A.R., and Hall, I.M. (2010). BEDTools: a flexible suite of utilities for comparing genomic features. Bioinformatics 26, 841–842.

Segal, E., and Widom, J. (2009). From DNA sequence to transcriptional behaviour: a quantitative approach. Nat. Rev. Genet. 10, 443-456.

Singh K, Talla A, Qiu W. (2012). Small RNA profiling of virus-infected grapevines: evidences for virus infection-associated and variety-specific miRNAs. Functional & integrative genomics 12: 659–669.

Sorin, C., Declerck, M., Christ, A., Blein, T., Ma, L., Lelandais-Briere, C., Njo, M.F., Beeckman, T., Crespi, M. and Hartmann C. (2014). A miR169 isoform regulates specific NF-YA targets and root architecture in Arabidopsis. New Phytologist 202, 1197-1211.

Sunkar, R. and Jagadeeswaran, G. (2008). In silico identification of conserved microRNAs in large number of diverse plant species. BMC Plant Biology, 8, 37

Szittya, G., Silhavy, D., Molnár, A., Havelda, Z., Lovas, A., Lakatos, L., Bánfalvi, Z., and Burgyán, J. (2003). Low temperature inhibits RNA silencing-mediated defence by the control of siRNA generation. EMBO J. 22, 633-640.

Trapnell, C., Roberts, A., Goff, L., Pertea, G., Kim, D., Kelley, D.R., Pimentel, H., Salzberg, S.L., Rinn, J.L., and Pachter, L. (2012). Differential gene and transcript expression analysis of RNA-seq experiments with TopHat and Cufflinks. Nat. Protocols 7, 562–578.

Vazquez, F., Vaucheret, H., Rajagopalan, R., Lepers, C., Gasciolli, V., Mallory, A.C., Hilbert, J.L., Bartel, D.P., and Crété, P. (2004). Endogenous trans-acting siRNAs regulate the accumulation of Arabidopsis mRNAs. Mol. Cell 16, 69-79.

Voinnet, O. (2009). Origin, biogenesis, and activity of plant microRNAs. Cell 136, 669-687.

Wierzbicki AT, Ream TS, Haag JR, Pikaard CS. 2009. RNA polymerase V transcription guides ARGONAUTE4 to chromatin. Nat Genet 41: 630–634.

Xie, Z., Allen, E., Wilken, A., and Carrington, J.C. (2005). DICER-LIKE 4 functions in trans-acting small interfering RNA biogenesis and vegetative phase change in Arabidopsis thaliana. Proc. Natl. Acad. Sci. USA 102, 12984-12989.

Yoshikawa, M., Peragine, A., Park, M.Y., and Poethig, R.S. (2005). A pathway for the biogenesis of trans-acting siRNAs in Arabidopsis. Genes Dev. 19, 2164-2175.

Zhao M, Ding H, Zhu JK, Zhang F, Li WX. (2011). Involvement of miR169 in the nitrogen-starvation responses in Arabidopsis. New phytologist 190: 906–915.

Zhong X, Du J, Hale CJ, Gallego-Bartolome J, Feng S, Vashisht AA, Chory J, Wohlschlegel JA, Patel DJ, Jacobsen SE. 2014. Molecular mechanism of action of plantDRMde novoDNAmethyltransferases. Cell 157: 1050–1060.